ULTRA WIDE GAP BRAZING OF HIGH TEMPERATURE

CAST STEEL BOILER VALVES

by

Christopher Wilkins

ProQuest Number: 10795216

ProQuest 10795216

A thesis submitted to the Faculty and the Board of Trustees of the Colorado

School of Mines in partial fulfillment of the requirements for the degree of Master of

Science (Metallurgical and Materials Engineering).

Golden, Colorado

Date: 4-12-10

Signed: _____
Christopher Wilkins

Signed: _____
Dr. Stephen Liu
Thesis Advisor

Golden, Colorado

Date: 4-12-10

Signed: _____
Dr. Michael Kaufman
Professor and Head
Department of Metallurgical and Materials Engineering

ii

ABSTRACT

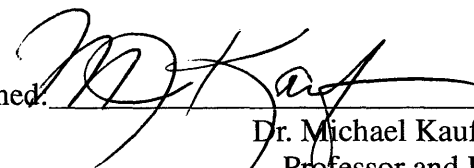Repair of large, high temperature components such as boiler valves in the electric power industry is often difficult and time consuming. Currently most repairs are carried out using welding processes which require skilled technicians and significant time investments. Therefore, alternate repair methods are of significant interest to the industry. An experimental investigation was carried out to evaluate the feasibility of braze repairing cracks in high temperature cast steel boiler valves. In addition, the braze repair process was characterized to understand in depth the filler metal flow and wetting phenomena which are involved. A custom nickel based filler metal alloy was developed and tested along with a commercial silver based brazing filler metal. The physical properties of the nickel based alloy were then determined. Also, a chemical cleaning process for heavily oxidized boiler parts was refined and its effectiveness was verified using actual valve specimens. Subsequently, cracked samples were brazed and a brazing procedure was established. The resulting braze repairs were then characterized using metallography, light optical microscopy, and scanning electron microscopy. The repairs were determined to be of good quality and suitable for use in boiler valve repair applications. Finally, analysis was performed regarding the unique aspects of ultra wide gap brazing, such as unique flow behavior that deviates from surface tension driven flow. A technique was proposed to mitigate the primary limitations of ultra wide gap brazing in crack repair applications.

TABLE OF CONTENTS

LIST OF FIGURES

vii

LIST OF ABBREVIATIONS

cfh – Cubic feet per hour

DTPA – Diethylene-Triamine-Pentaacetic Acid

EDS – Energy Dispersive Spectroscopy

EPRI – Electric Power Research Institute

SEM – Scanning Electron Microscopy

LIST OF TABLES

ACKNOWLEDGEMENTS

PREFACE

The motivation for this body of work is the mitigation of an issue related to boiler valves and commonly found in the electric power industry. Subjected to high temperatures, corrosive environment and high stresses, boiler isolation valves often experience cracking on their inner surfaces. While a current solution exists for repairing these cracks using a welding process, it is by no means ideal. Therefore, work has been performed to explore ultra wide gap brazing as a possible alternate solution. The primary focus of work was to determine the flow and defect formation mechanisms present in ultra wide gap brazing. In addition, it was also necessary to determine the appropriate methodology to prepare the cracks for brazing and characterize the brazing process in depth.

CHAPTER 1

LITERATURE REVIEW AND BACKGROUND INFORMATION

An understanding of the boiler valves of interest as well as the unique properties

of brazing is important before engaging upon a research project.

1.1 Boiler Valves

In the electric power industry, coal-fired power plants contain numerous parts in

the boiler loop that experience high temperatures. Many points on the boiler loop are

exposed to elevated temperatures as well as water or steam. In either case the

combination of heat and moisture creates substantial oxidation on the interior surfaces of

these components. Of interest in this study are boiler isolation valves, referred to here as

boiler valves. These components are typically made of low alloy cast steels with wall

thicknesses ranging from three to twelve inches. Each valve weighs several tons and

consists of a large cast steel valve body and a valve insert. Repair of the valve body itself

is of specific interest within this investigation. As earlier indicated, within the boiler

assembly, boiler valves are exposed to both elevated temperatures and oxidizing

environments, as well as mechanical stresses. As a result of the heat and aggressive

environment, the interior surfaces of boiler valves quickly become oxidized. In addition

to normal oxidation, the added stresses created by the elevated operating pressures can

create stress corrosion cracking on the interior surface as shown in Figure 1.1.

Upon prolonged exposure to high service temperature and corrosive environment,

the entire interior of a boiler valve eventually becomes covered in a network of shallow

4
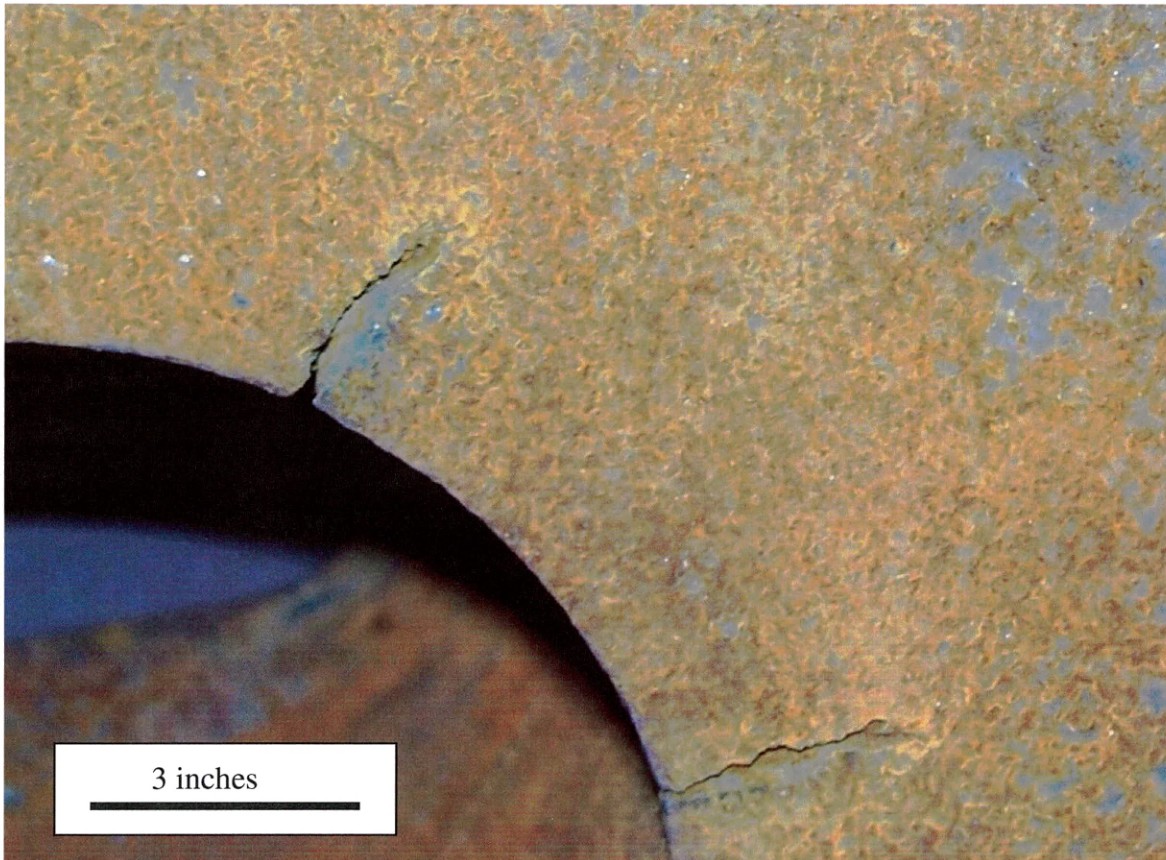
Figure 1.1 – Cracked boiler valve specimen showing major cracks radiating from the interior surface of the valve [2]

stress corrosion cracks such as those shown in Figure 1.2, which are not considered to be detrimental to the long-term life of the part. However, some of these cracks may continue to extend into the valve body turning into significant defects that must be repaired. Currently repairs are conducted using a welding process that requires the removal of the entire crack, filling the resulting cavity with weld metal, and stress relieving the entire valve. This repair procedure is highly costly due to the size of the parts involved and the complexity of the weld repair. In addition, the welding process can result in deformation in the boiler valve, which can be detrimental to proper function. [1]

2 inches

Figure 1.2 – Interior valve surface showing network of shallow cracks covering entire interior surface [2]

It was decided that a brazing repair technique may have the capability of repairing cracks in boiler valves using less time, thus reducing overall repair costs. The results of a study examining all aspects of brazing in this application are presented in this thesis.

The boiler valves of interest are composed of cast low alloy steel. While compositions may vary, a typical composition of the cast steel is given in Table 1.1. Due to the presence of a cast microstructure, any welding repair process may cause significant changes in the microstructure and thus mechanical properties of the weld as well as mechanical distortion. These changes remain even after stress relieving heat treatments. In addition, heat treatments can cause microstructural transformations in areas outside of

the weld-metal region. The changes in mechanical properties of the boiler valve will likely shorten the useful life of the valve.[2]

Table 1.1 Nominal boiler valve alloy composition (in wt.%)

Fe	C	Si	Mn	Cr	Cu	Ni
Balance	0.08	0.4	0.9	0.3	0.3	0.3

1.2 Conventional Brazing

Brazing is a well established non-fusion metal joining process with many diverse applications. In brazing, components are joined together using a dissimilar filler metal (when compared with the base steel) which has a lower melting point than the base metal but higher than 450 °C as defined by the American Welding Society. The filler metal is melted and introduced into the joint while the base metal remains solid. When cooled, the filler metal adheres to the base metal, forming a sound joint. [3] The gap width of traditional brazed joints is around 0.005 inches (0.13 mm), however the gap width of the ultra-wide gap joints considered in this work is 10 to 20 times wider, between 0.05 and 0.1 inches (1.3 and 2.5 mm). Joints with gap width between 0.005 and 0.05 inches (0.13 and 1.3 mm) are considered wide gap joints for the purposes of this work.

There are many brazing filler metals from a number of alloy systems for different applications. Some examples are copper based alloys, nickel based alloys, and silver based alloys. Selection of a specific alloy composition for brazing is based primarily on its melting point, surface tension, fluidity, wetting, and coefficient of thermal expansion

(CTE). Melting point is significant because the filler metal must flow at a temperature low enough that the base metal does not exhibit significant metallurgical changes. In addition, the melting point must be high enough that the filler metal maintains mechanical strength at service temperature. Finally, in many cases the relative thermal expansion coefficients of the filler metal and base metal are important. If the CTE mismatch is too great additional stresses can develop within the joint which can lead to reduced joint strength. To overcome this problem, filler metals are often selected to match the CTE of the base metal as close as possible.

Surface tension is one of the most significant properties of a brazing filler metal. In conventional brazing filler metal flow is driven by the relative surface tension of the filler metal and base metal. When the covering of a base metal by a filler metal is accompanied by a total reduction in surface energy, that energy reduction acts as the primary driving force for filler metal flow. The energy balance is most easily expressed graphically using a diagram of a sessile drop, which is a molten drop of liquid on a flat surface, shown in figure 1.3. Each arrow on the diagram represents one component of the total surface energy of the system. The surface energy interactions cause the formation of an equilibrium contact angle, θ, which is an important indicator of the wetting between a liquid and solid. The surface tension difference draws the filler metal into the joint and has the capability of drawing filler metal long distances and against the force of gravity. This flow is known as capillary flow and is one of the most important characteristics of traditional brazing. [4]
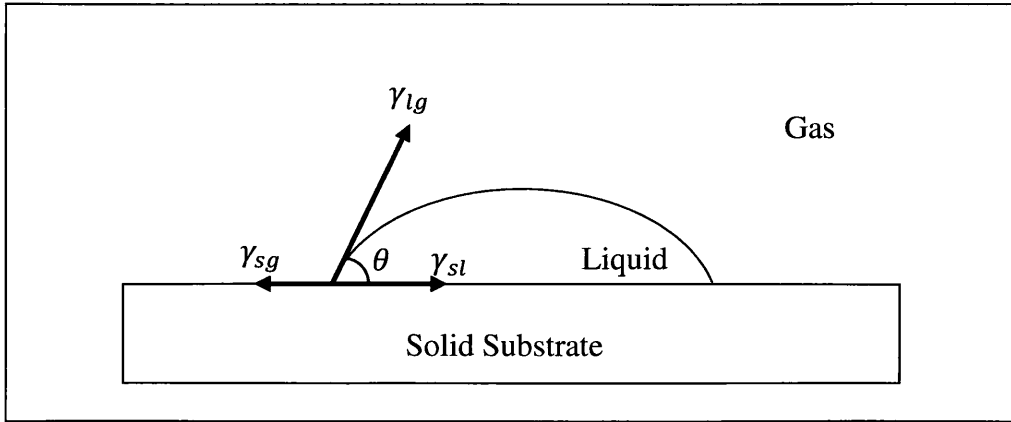
Figure 1.3 – Diagram of a sessile drop showing surface energy vectors and wetting angle

Fluidity is significant in brazing because brazed joints commonly have complex

geometries and close tolerances. The filler metal must flow sufficiently well that it can

reach all areas of the joint and form a clean interface across the entire joint. In addition,

high fluidity filler metal is also desirable for manual brazing characteristics. Fluidity is

the inverse property of viscosity, one of the primary properties of a liquid. The

constitutive equation governing viscosity and fluidity for Newtonian fluids is given in

Equation 1.1, where τ is the viscosity, μ is the coefficient of viscosity, and $\dfrac{du}{dy}$ is the

velocity gradient of the fluid. [5,6]

$$\tau = \mu \frac{du}{dy} \tag{1.1}$$

The compatibility between filler metal and base metal is significant to the overall

quality of the brazed joint. The most basic measure of compatibility between filler metal

and base metal is wetting. The ability of a filler metal to wet a base material is

determined by the surface tension between the two materials, as well as the surface

tension between each of those materials and the atmosphere. This interaction is defined

by Young's equation, Equation 1.2, where γ_{ls} is the liquid/solid surface tension, γ_{lg} is the

liquid/gas surface tension, γ_{sg} is the solid/gas surface tension and θ is the wetting angle.

When θ is greater than 90 degrees the liquid is considered to not wet the solid. In order

for a filler metal to flow, it must wet the solid; wetting angles smaller than 60 degrees are

preferred when selecting a filler metal.

$$\gamma_{sg} - \gamma_{ls} = \gamma_{lg}cos\theta \tag{1.2}$$

As brazed joints are typically composed of dissimilar materials it is common that

reactions occur between the filler metal and the base metal. These reactions can either be

detrimental or beneficial depending on the material system. One common reaction that

can occur is dissolution of the base metal when the base metal has significant solubility in

the molten filler metal. In addition, for substantial dissolution to occur the brazing cycle

must be long enough that the kinetics of dissolution becomes favorable. Dissolution can

have detrimental effects on a joint and must be evaluated carefully, particularly when

long brazing processes such as furnace brazing are used.

Another common reaction to occur is the formation of intermetallic compounds at

the interface. The formation of intermetallic compounds generally increases the

wettability of the filler metal on the base metal. Therefore in situations where the base

metal is difficult to wet, it is common to select a filler metal which will react to form an

intermetallic compound. [7] Caution must be taken, however, when selecting a materials

system which forms intermetallic compounds since they are generally hard and brittle, and therefore detrimental to the overall joint performance. Intermetallic compounds are therefore commonly avoided in situations where joint strength is important.

Brazed joints are commonly tested in several ways. The overall joint strength is usually tested by shear testing of a lap joint. Since brazed joints are not typically placed in tension, tensile testing is not commonly used for evaluating brazed joints. Joints are also sectioned to evaluate the interface between the filler metal and base metal. In this case both the wetting between the filler metal and base metal as well as the exact nature and microstructure of the interface between the filler and base materials can be characterized. Good quality brazed joints have little to no porosity at the interface and exhibit a continuous interface without inclusions. Finally, sectioning can help evaluate the joining process regarding intermetallic compound formation.

1.3 Wide Gap Brazing

Conventional brazing requires very narrow and consistent gap widths for success. Preparing brazed joints can be time consuming and costly due to tight mechanical tolerances within the joint, therefore decreasing the requirements of the tolerances is of interest. The easiest method of reducing joint preparation requirements is to increase the acceptable gap width for brazing. This technology is known as wide gap brazing.

Wide gap brazing is a relatively new concept and requires several unique considerations. In conventional brazing the mechanical strength of the filler metal does

not have a substantial impact on finished joint strength. In wide gap brazing, the filler metal must have sufficient mechanical strength to form a strong joint.

In addition, the filler metal must be able to flow well into the joint. Due to the wider joint and the larger mass of the filler metal present, the surface tension contribution to the flow behavior becomes smaller. As a result, complete joint filling becomes more difficult because the filler metal may not be able to easily flow vertically as it can in traditional brazed joints. As such, joint designs for wide-gap brazing commonly make use of gravity to assist filler metal flow.

The increased joint gap of wide-gap brazing also has consequences when using very high fluidity filler metals. High fluidity filler metals such as pure metals will sometimes have difficulty bridging the entire joint gap. With sufficient fluidity, the molten filler metal may not come into contact with both sides of the joint during brazing. It has been found that filler metals with wider melting ranges are better able to fill the wider joints because they can remain partially mushy during flow, creating increased contact between the filler metal and joint walls. In addition, filler metals with wider melting ranges have been found to reduce shrinkage porosity in certain joint configurations.

CHAPTER 2

EXPERIMENTAL PROCEDURES

To evaluate the feasibility of braze repair of ultra-wide gap cracks in boiler valves, a series of experiments was performed. After feasibility was established, the resulting joints were examined to characterize their properties and determine their suitability for the boiler environment. This section contains the experimental approach used to accomplish the evaluation and process development.

2.1 Crack Characterization

In order to properly repair cracks in boiler valves, the exact morphologies of the cracks must first be characterized. Several methods were considered to accomplish this task. Visual examination, ultrasonic examination, and replication by casting were selected as the most promising methods of characterizing the existing cracks.

Multiple boiler valve samples were obtained from EPRI for further testing. They contained surface cracks that exhibited a variety of crack morphologies. The majority of the samples were covered with a network of small, shallow cracks as well as a smaller number of significantly deeper cracks, referred to as primary cracks. Each sample was first photographed and the most significant cracks were visually identified. These primary cracks were then probed using thin wires to form a rough depth profile. Subsequent examination was conducted to provide more complete dimensional information for all cracks on the samples.

In addition to the samples obtained from EPRI, several phased array ultrasonic scans of more severe cracks than those present in the physical samples were also provided by EPRI. These ultrasonic images supplied detailed information on the maximum dimensions of cracks to be considered. From the ultrasound scans a nominal depth of 1.5 (38 mm) inches and width of two inches (50 mm) was selected for the size of the test specimens for crack replication. It should be noted that these dimensions are not those of the physical samples obtained from EPRI, but instead those of cracked samples which remained in the possession of EPRI and from which the ultrasonic images were produced.

The dimensions determined by ultrasound suggest that the cracks in the physical samples must be characterized in greater detail than simple surface examination. Casting was selected as a method to gain a detailed replica of the cracks of interest. The initial casting material tested was a low temperature solder. While the solder was able to be melted on the cracked surfaces, it did not penetrate into the cracks to any significant depth. Instead, the solder balled up as illustrated in Figures 2.1 and 2.2. This observation is not surprising because of the thick oxide layer on the valve samples that creates non wetting conditions for the molten solder. In an attempt to alleviate this problem, a fluxed solder was used. However, the volume of oxide present in the crack was far too significant to be removed by fluxing action. As a result, solder was disqualified as a viable casting material for this application.
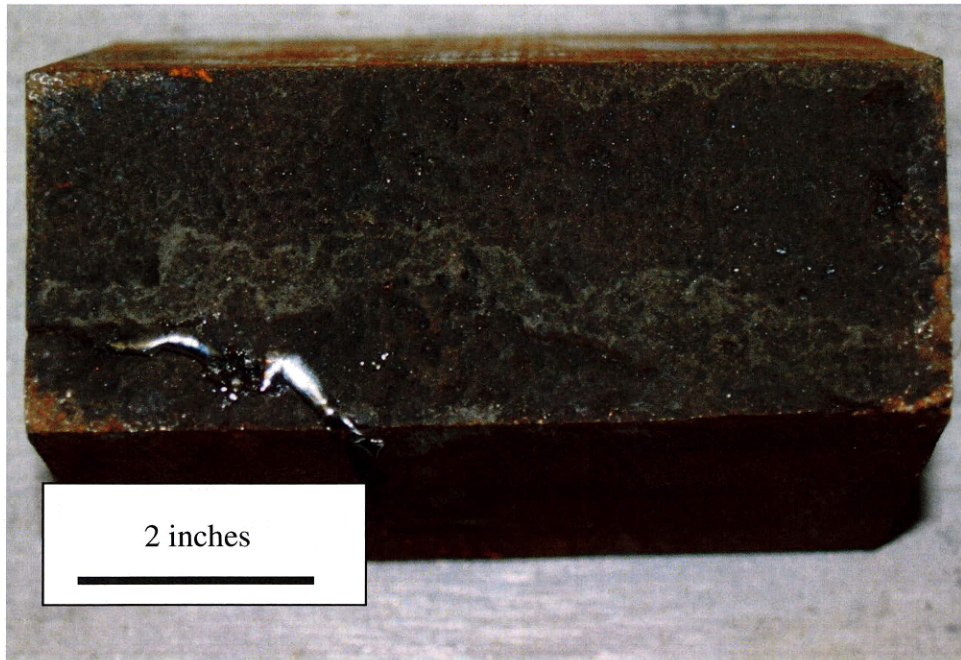
Figure 2.1 – Solder cast in place at surface of boiler valve crack

An alternate material considered for crack casting was acrylic. Small amounts of clear acrylic were dissolved in acetone up to the solubility limit. At this point the dissolved acrylic solution was very viscous and wet the oxidized steel surfaces very well. The solution was placed into the cracks and then allowed to cure. The cast appeared to fit the crack well with good penetration. Difficulty was encountered, however, when attempting to remove the casts from the cracks. The casts bonded strongly to the existing cracked surfaces such that they shattered into small plastic shards when attempting to remove the casts from the cracks.
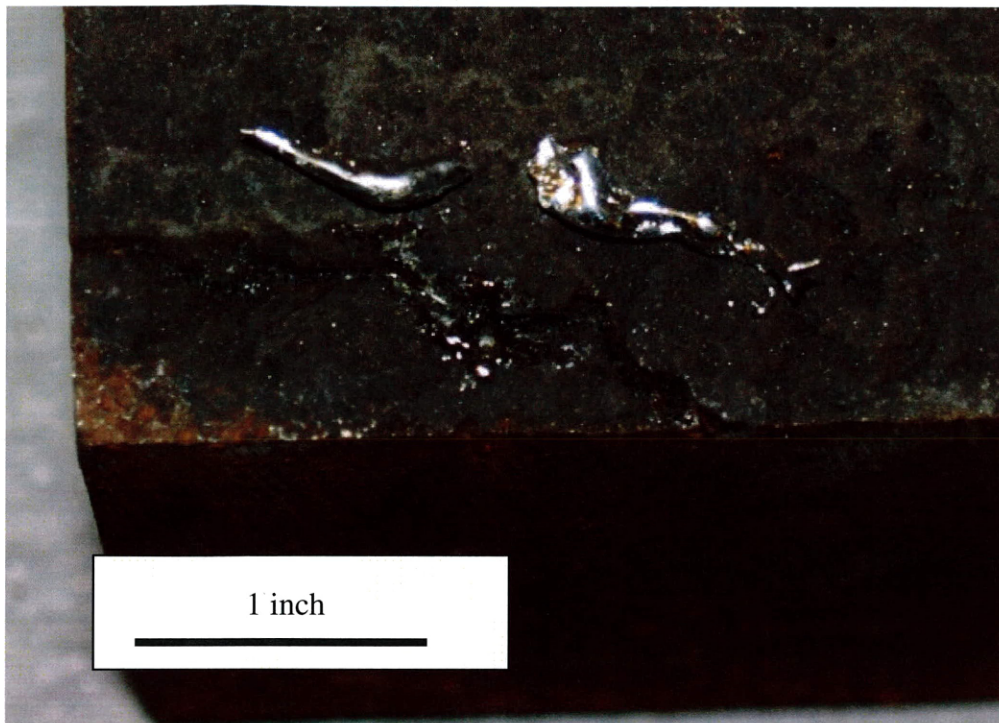
Figure 2.2 – Solder cast removed from crack and shown inverted, cast shows lack of penetration into crack root and poor replication of crack morphology

The shards were small enough that it was not possible to reassemble them into a negative version of the crack in question, offering no details regarding the crack morphologies. Therefore, it was determined that acrylic was not a viable casting material for crack characterization.

Taking lessons from previous casting attempts, it was determined that several characteristics were required of a successful casting material. Flexibility, dimensional stability, and good wetting on the cracked surfaces were the most important properties for this application. After research, a material known as Mikrosil™ was found to exhibit the characteristics sought. Mikrosil™ is a forensic casting material used for tool mark identification. It is supplied as two separate pastes which are mixed before casting, in a

similar way to many epoxies. Once cured, the material remains flexible and rubbery and can be easily removed from steel surfaces without the need of any mold release. Because of these characteristics, a sample of Mikrosil™ was ordered for testing. For ease of photography, gray colored Mikrosil™ was chosen. For each sample, a small quantity of Mikrosil™ was prepared and worked by hand into the cracked surface using a small spatula. After curing, the Mikrosil™ cast was removed from the cracked surface using a dental pick for examination and characterization of all cracks present on the sample.

The Mikrosil™ casts were examined using optical microscopy, scanning electron microscopy, and visual examination. Each cast was also directly compared to the original boiler valve sample in order to directly identify the cracks present.

2.2 Filler Metal Development

In order to repair the cracks of interest, an appropriate filler metal must be selected for the application. As observed in other brazing processes, the filler metal must exhibit several primary characteristics that are critical to the formation of a quality brazed joint. The filler metal must wet the base metal well. Also, the filler metal must have adequate fluidity to flow to all areas of the crack. The melting temperature of the filler metal must be sufficiently higher than the service temperature of the part so that it retains those properties required of the joint. However, the melting temperature must also be low enough that the base metal does not reach its melting point or a specified maximum temperature during brazing. In this case the maximum temperature was determined to be the A1 temperature for the boiler valve steel of approximately 725°C. In addition, the

filler metal must be metallurgically compatible with the base metal. Finally, the brazed joint, i.e. the solidified filler metal and its interface with the base metal, must perform well in service after repair.

Commercial filler metals were first considered as possible candidates. The BNi series of alloys was considered most promising due to their high service temperature capabilities, high mechanical strengths and excellent adhesion to steels. Further examination of BNi alloys, however, highlighted a major concern in this particular application. First, both phosphorus and boron are common alloy additions to nickel based brazing alloys that could cause embrittlement in steels. It should be noted that their presence does not normally cause problems for joints in low temperature service. This behavior is because in low temperature service there is not sufficient mobility for diffusion of the elements into the substrate to occur.

At the service temperature of boiler valves elements such as boron and phosphorus exhibit high mobility that would allow significant infiltration of both elements into the steel adjacent to the brazed joints. Additionally, the levels of both elements present in B-Ni alloys are substantial enough to possibly compromise the long term stability of the brazed boiler cracks.

Due to the other promising properties of B-Ni alloys it was determined that a new nickel based alloy should be designed that would contain lower levels of phosphorus and completely eliminate boron. To accomplish this objective, the first step was to perform

theoretical calculations using Thermo-Calc software to understand the roles of various

alloying elements in the nickel system. To this end, Thermo-Calc was used to generate

several pseudo-binary phase diagrams, one of which is shown in Figure 2.3, each

examining the role of a single alloying addition in the system of interest.
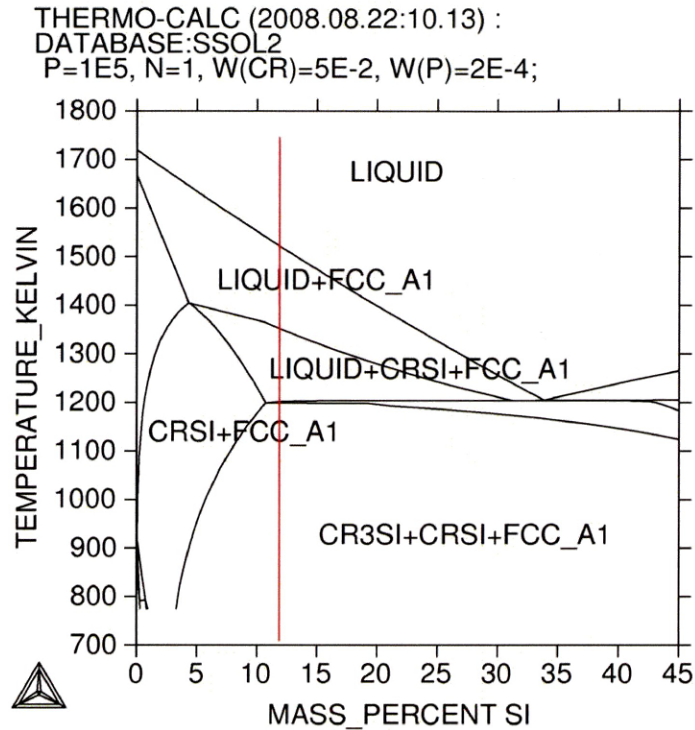
Figure 2.3 – Calculated pseudo-binary phase diagram showing effect of silicon on nickel based filler metals. Red line shows approximate composition of alloys tested.

It was determined that phosphorus is a strong melting point depressant for nickel

and likely could not be completely eliminated without creating an alloy with too high of a

brazing temperature. In addition, silicon was shown to have melting point depressant

properties, although a much higher concentration would be required for a significant

effect. Finally, carbon was examined and was shown not to have a substantial effect on

the melting behavior of the alloy. However carbon was still included in the created alloys in order to increase mechanical strength and reduce the possibility of carbon depletion of the valve metal near the crack by diffusion. In addition, chromium was included as an alloying element due to its effect on improving corrosion resistant properties, predicted to be critical to the long term survival of the repairs in service.

A series of alloy compositions was then developed using the Thermo-Calc software package as a basis for theoretical predictions. The alloys were then produced in-house and tested for suitability. Initial production of brazing filler metal alloys presented a challenge in that it was necessary to produce the alloys in small quantities with precise compositions. The first method considered for production was powder mixing. High purity metal and alloying powders were measured using an analytical balance and then mixed manually. The powder mixtures were subsequently placed in a ceramic crucible in a controlled atmosphere furnace. Ultra high purity argon (99.999 % pure) flowed through the furnace continuously at a rate of 4.5 cfh. The powder mixture was then heated to 1175 °C and held at temperature for two hours. The temperature was selected as the maximum temperature allowable for brazing. The furnace was then allowed to cool to room temperature slowly. After examining the cooled powder mixture, it was apparent that no meaningful consolidation occurred. Although some particles did sinter together, this sintering did not produce a uniform alloyed droplet as required for subsequent testing.

As an alternate method for producing filler metal samples, the use of a button melter was examined. In this method the powders were initially prepared in the same way as described in the last paragraph and combined into a mixed powder sample. This powder mixture was then placed into the button melter, which is basically a gas tungsten arc welding (GTAW) system surrounded by a protective enclosure as shown in Figure 2.4. In this case, the enclosure was filled with flowing high purity argon to prevent oxidation. In addition, a water cooled copper substrate was used to ensure that only the filler metal was melted. The GTAW process quickly melts the powders followed by solidification. After the arc was extinguished the solidified button of filler metal was allowed to cool under the protective atmosphere. The resulting alloyed samples were used for all subsequent testing and analysis of the custom filler metal alloys.

To confirm the predicted properties of the custom designed alloy, differential scanning calorimetry (DSC) was utilized. A small sample of the consolidated alloy with a mass of less than a gram was placed in a ceramic crucible. The sample was then heated to melting under argon and then allowed to cool at a constant rate. As the sample was cooled, the heat flow into and out of the sample was compared to an empty reference crucible. The heat flow events were then examined to determine the temperature of solidification as well as to identify any unexpected phase changes.
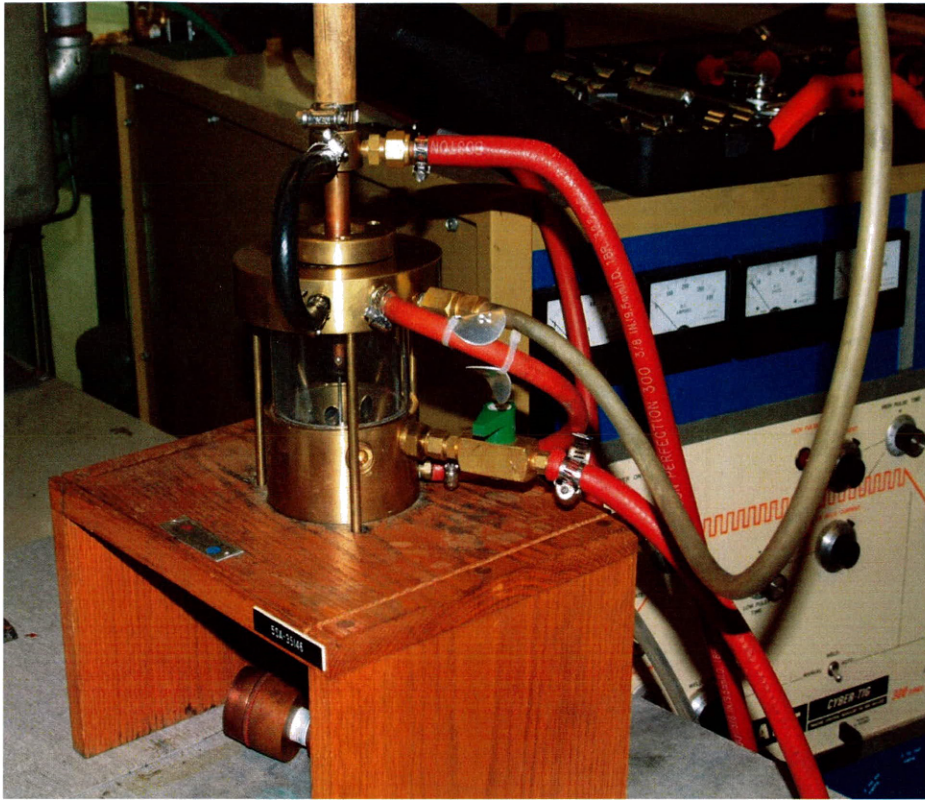
Figure 2.4 – Button melter used to produce custom filler metal samples. Apparatus consists of GTAW welder surrounded by a protective enclosure.

After the custom filler metal alloys were produced, a series of examinations were performed to determine their properties as filler metals. The primary properties of interest were wetting angle, spreadability, and chemical reactivity with the base metal. As mentioned earlier, the viscosity of the molten filler metal was not characterized in this work. The primary test used to examine the selected properties was a sessile drop test, in which a small button of filler metal was placed on a prepared base plate and then melted. The base material selected for the sessile drop tests was ASTM A-36 steel, which is sufficiently similar to the low alloy steel used in boiler valves that qualitative comparisons should be possible. All base metal samples were ground clean of mill scale and manually ground to 600 grit to minimize surface texture effects. It should also be

noted that the ASTM A-36 steel selected was a wrought product as opposed to the cast boiler valves, however this discrepancy is not expected to cause significant differences in the properties being examined. Wetting and spreading are expected to be more macroscopic and surface-related phenomena. Solidification of the molten filler metal, on the other hand, would be expected to depend more on the substrate microstructure. Therefore the alloy composition of the steel substrate is far more important than its processing history.

Sessile drop tests were performed in a tube furnace heated using resistance heating elements shown in Figure 2.5. Flowing ultra high purity argon was used for the atmosphere in order to prevent oxidation. During the tests the argon flow was maintained at between 4.5 and 5.0 cfh. Each sample was heated to melting and maintained at that temperature until the wetting angle stabilized. It should be noted that samples B, C, and D did not melt at the maximum furnace temperature and therefore did not produce wetting angle data. The wetting angle was recorded using a high speed video camera adapted with a high magnification macro lens in order to observe any changes of the wetting angle with time and determine when equilibrium was achieved. The final equilibrium wetting angle was used for subsequent comparison. One image from the high speed video is shown in Figure 2.6 with the wetting angle indicated. The viscosity of the filler metal was not measured in this work.
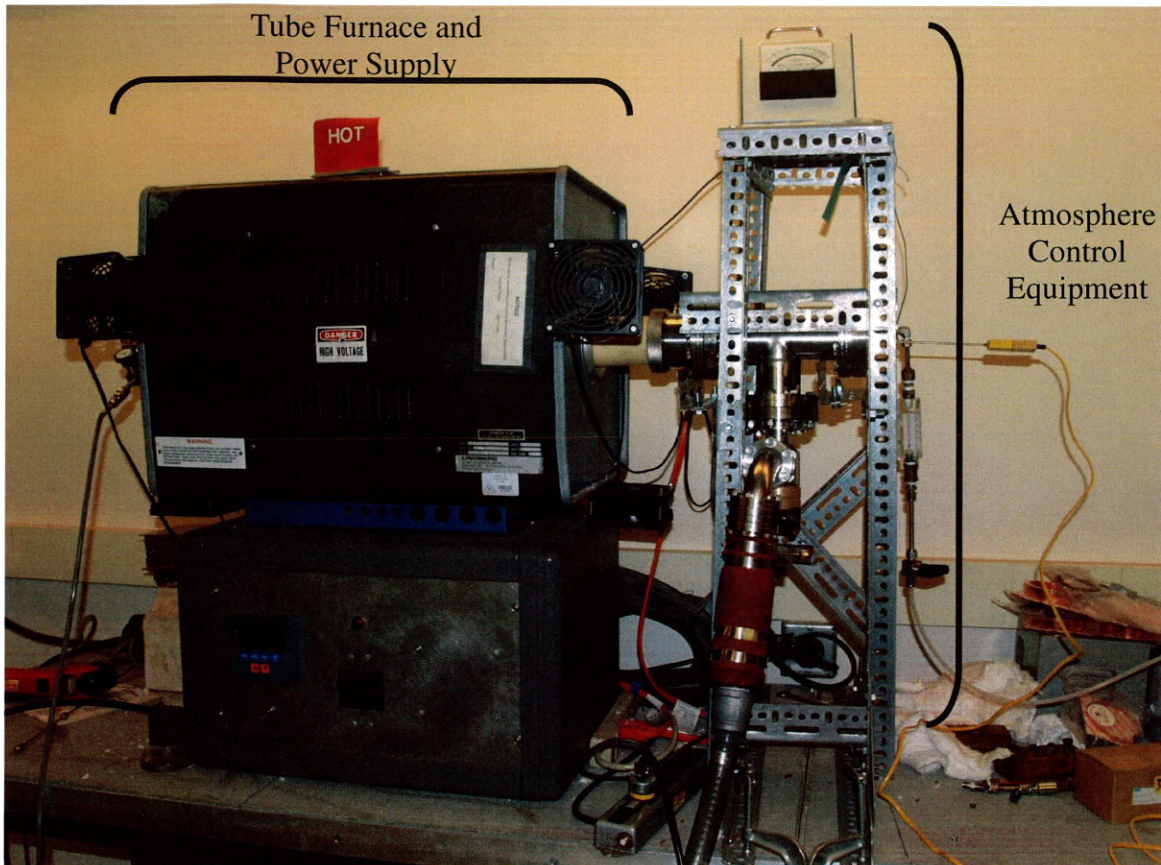
Figure 2.5 – Tube furnace and related atmospheric control equipment used for sessile drop tests as well as subsequent brazing tests.
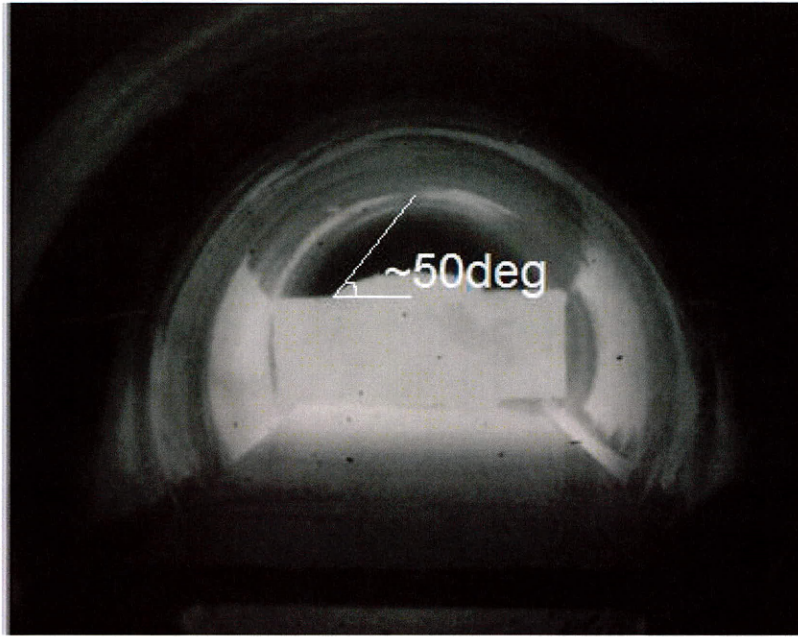
Figure 2.6 – Sessile drop showing wetting angle after filler metal flow has completed.

2.3 Flow Analysis and Defect Formation

To investigate the flow patterns of the molten filler metal and defects that form within ultra-wide gap joints, a series of semi-circular joints each with a blind crack were designed. Based on crack dimensions measured using the phased array ultrasound scans provided by EPRI [1], multiple crack shapes with varying length (W), depth (D) and width (G - gap dimension) were designed to simulate a variety of possible crack geometries found in the boiler valves, see Figure 2.7 and Table 2.1. Note the very long (44 mm) and deep (25 mm) cracks. The width is also quite large, greater than 2 mm. Comparing these numbers with the dimensions of cracks typically brazed, it is clear that the wide gap brazing process is unique such that it will require specially investigated filler metals.

Since it would be difficult to observe internal filler metal flow patterns at brazing temperatures, a secondary method was required to gain a thorough understanding of the mechanisms involved.
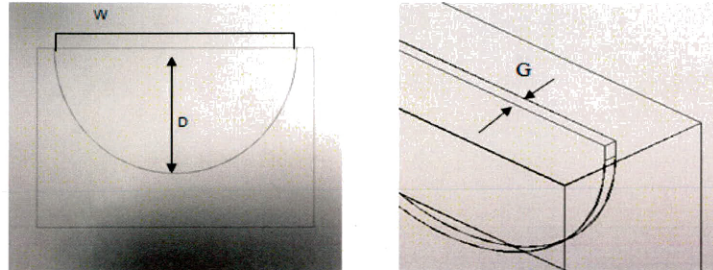
Figure 2.7 – Schematic of Sample Crack Geometry (W – crack length, D – crack depth, G - crack gap)

Table 2.1 Variations in Crack Geometry Used to Evaluate Flow Phenomena

Sample ID	W (mm)	D (mm)	G (mm)
1N	44	4.4	1.8
5N	44	13	1.8
9N	44	22	1.8
14N	28	25.0	1.8
1W	44	4.4	2.3
5W	44	13	2.3
9W	44	22	2.3
14W	28	25.0	2.3

A more effective method of examining the flow behavior would be to select a surrogate material system that flows at room temperature from which a greater quantity of data could be obtained. To identify and select an appropriate set of surrogate materials, two primary properties were selected for comparison. First, the liquid-solid surface tension should be replicated in order to closely reproduce the surface tension driven component of the flow behavior. In addition, proper fluid viscosity must be

chosen to influence the pressure-driven flow behavior. [8] Regarding both properties, the room temperature surrogate material system must be comparable to the silver-steel system at elevated temperature.

After obtaining property data for steel and silver based filler metals at typical brazing temperatures from literature, the surrogate system selected was uncoated acrylic plate paired with a fifty percent water, fifty percent propylene glycol mixture. The wetting angle and viscosity of the surrogate system were within ten percent of the tabulated values for the Ag-Steel target system [3]. Comparison of the properties of the two material systems is shown in Table 2.2.

Table 2.2. Wetting Angle and Viscosity Data Used to Establish Correlation

Material System	Wetting Angle (deg.)	Viscosity (cP)
Silver on Steel	25 [9]	0.828 [10]
50% H$_2$0 50% Propylene Glycol on Acrylic	22 (experimentally determined)	0.79 [10]

It should be noted that the viscosity of the mixture between water and propylene glycol is not a simple average between their individual values. A multi-step process is required to determine what is referred to as the Refutas Equation. First, the viscosity blending number (VBN) is calculated for each liquid using Equation 2.1. [11]

$$VBN = 14.534 * \ln[\ln(v + 0.8)] + 10.975 \tag{2.1}$$

Next, the viscosity blending number of the mixture (VBN$_{Blend}$) is calculated using Equation 2.2. In this equation x$_N$ is the mass fraction of component N in the mixture.

$$VBN_{Blend} = [x_A * VBN_A] + [x_B * VBN_B] + \cdots + [x_N * VBN_N] \tag{2.2}$$

Finally, the blending number of the mixture is converted back to a viscosity by solving Equation 2.1 for v, which is shown in Equation 2.3. This method was used to calculate the mixture viscosity used for comparison. There is an additional method for determining the viscosity of a solution shown in Equation 2.4. [12]

$$v = \exp\left(\exp\left(\frac{VBN_{Blend} - 10.975}{14.534}\right)\right) - 0.8 \tag{2.3}$$

$$\mu \approx \frac{1}{x_a/\mu_a + x_b/\mu_b} \tag{2.4}$$

All flow tests using the surrogate material system were conducted at room temperature. Multiple trials were conducted for each joint geometry to establish statistically significant results. The fluid was introduced at the right hand edge of the joint, taking between 5 and 9 seconds to fill the entire joint. Each joint was filled to the top. The flow process was recorded using a high speed imaging system at 250 frames per second. Information regarding behavior when a joint is only partially filled can be obtained by observing the initial portions of video which is recorded.

The liquid velocity in the cracks was deliberately varied by manually altering the introduction rate of the fluid into the crack mouth in order to examine the influence of flow velocity on advance mechanism. Multiple trials were conducted ranging from very slow (0.25 cm/sec) to very fast (18 cm/sec) inflow rates that scaled with the interface velocities observed on high speed video. There was no specific target flow velocity selected for the trials. Instead, it was decided that a large number of different velocities ranging from slow to fast should be tested. The slowest velocity was defined as the lowest rate at which fluid could be introduced in a stable manner. The fastest velocity was determined by the inflow rate which would cause sufficient turbulence in the fluid to prevent stable flow.

2.4 Crack Preparation

Due to the presence of a thick oxide layer on the cracked surface, a cleaning procedure was required to remove the oxides prior to brazing. Two primary cleaning techniques were used to accomplish this goal. First, mechanical cleaning was used to reduce the total oxide volume. The top surface was cleaned using a wire brush and compressed air until all loose oxides were removed. Mechanical cleaning would be followed by chemical cleaning to completely remove the oxide layer.

A candidate chemical cleaning procedure was suggested in the EPRI crack cleaning document [2]. This procedure consisted of immersing the sample in hydrogen peroxide for 60 seconds, and then immersing the sample in a cleaning solution until the oxide layer is removed as shown in figure 2.8. The cleaning solution was prepared by

dissolving Diethylene Triamine Pentaacetic Acid (DTPA) to maximum solubility in 3 pct.

hydrogen peroxide and ammonium hydroxide. The ammonium hydroxide was used to

adjust the pH of the solution to a slightly basic value (typically between 8 and 9). The

cleaning procedure was then optimized experimentally in order to successfully clean the

cracked surfaces and prepare samples for the brazing trials.
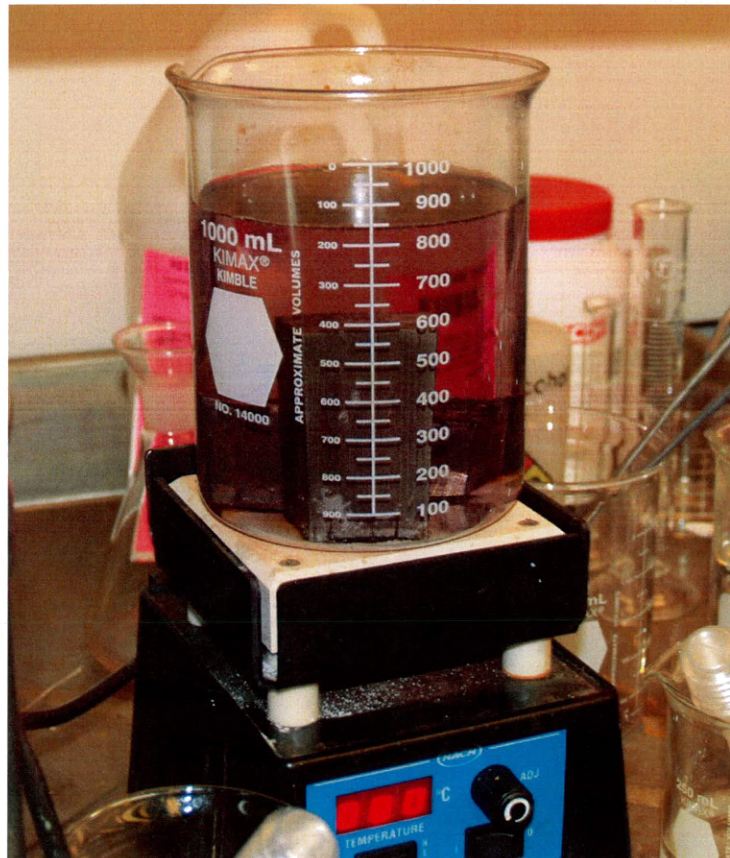
Figure 2.8 – Laboratory setup used for chemical cleaning of boiler valve samples.
Samples are immersed in cleaning solution and then heated to 80°C

2.5 Brazing Repair Procedure Development

Once cleaning was complete, it was determined that the cracks were ready for

brazing trials. It was decided that both the custom nickel based filler metal alloy as well

as the selected silver based alloy would be used in the initial brazing tests. The silver

based filler metal was obtained commercially in the form of wires.

To evaluate brazing of the cracked surfaces, multiple samples were cut from the

cracked specimens provided by EPRI. Sample dimensions were approximately 1 inch X

1 inch X 1 inch (25 mm X 25 mm X 25 mm). Each sample was then cleaned using the

oxide removal procedure detailed in the previous section. After cleaning was complete,

each sample was immediately brazed in the tube furnace under parameters detailed

earlier.

2.6 Repair Property Determination

The quality and properties of the resulting repair is important to the success of the

entire repair procedure. As such, several properties of the completed repairs were

experimentally determined. The most significant property of concern is the degree of

wetting between the filler metal and base metal because any pores or other defects along

the wetted interface can act as initiation points for failure of the repair. To determine the

number of defects at the interface, multiple sections were taken from the repaired cracks.

Both transverse and longitudinal sections were obtained to account for any directional

preference of defects. Each section was then ground and polished by hand to one micron

diamond polish. Samples were then examined using optical and electron microscopy to

determine the extent of flow and the flow properties. In addition, brazed samples were

chemically cleaned using the oxide removal technique in order to determine the ability of

the repairs to survive subsequent cleanings.

CHAPTER 3

RESULTS AND ANALYSIS

After the conclusion of experimental work the whole project was evaluated to determine suitability of the established repair procedure for real world boiler valve cracks. In addition, a method was proposed to improve the versatility of the repair procedure which was established.

3.1 Crack Characterization

Surface examination showed that the primary cracks were of fairly consistent depth and were much shallower than they were long. A thin wire probe was used to measure the depth along the major cracks with an average depth of 3 mm and a maximum depth of 5 mm. It should be noted that the depths measured are not the actual crack depths but the depth measured to a specific width determined by the wire probe, in this case 0.5 mm.

As described in an earlier section, a thin layer of the mixed Mikrosil™ was worked into the cracks on the surface of a boiler valve sample. After curing, the cast was carefully removed from the surface with the assistance of a small metal dental pick. The cast was examined and was determined to be a good quality representation of the cracked surface. Complete flow to crack root over the extent of the sample was observed. The cast was photographed using oblique lighting as shown in Figures 3.1 to provide a visual record of the crack morphologies. Figure 3.2 is a photograph of the

cracked surface of the boiler valve. In addition, some casts were imaged using Scanning

Electron Microscopy (SEM) to produce images with greater depth of field and

magnification than was possible using light microscopy.
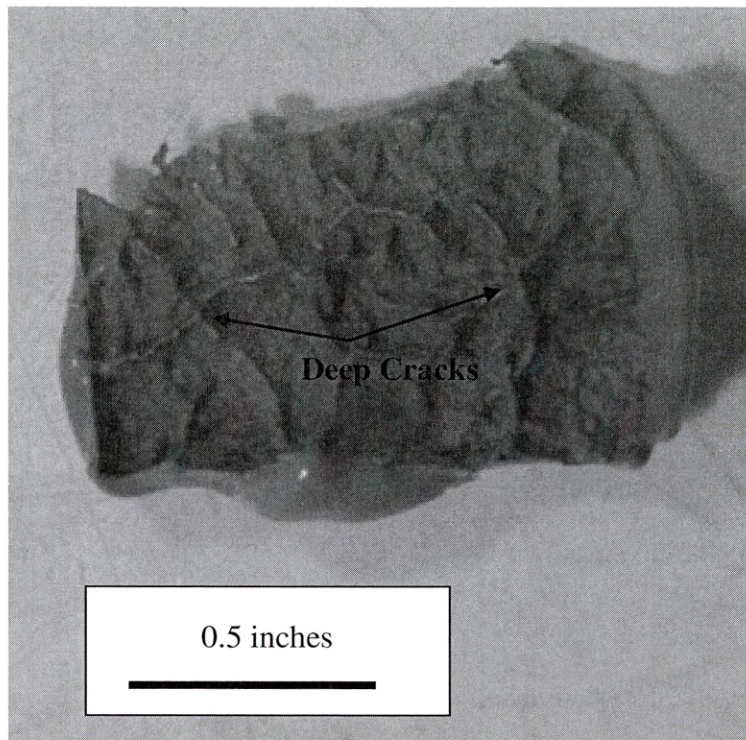
Figure 3.1 – Mikrosil™ cast of cracked surface photographed using oblique lighting. Cast shows complete flow to crack root over the extent of the sample. A number of deep cracks are also shown.

It became obvious that the network of cracks present on the valve surface was far

more complex than was evident from surface examination. Even though it was not

possible to conclusively determine the mechanism for crack formation from examination

of the resulting cracks, some hypotheses regarding crack propagation patterns were

established. Figures 3.3 and 3.4 show the interface between two adjacent cracks. The
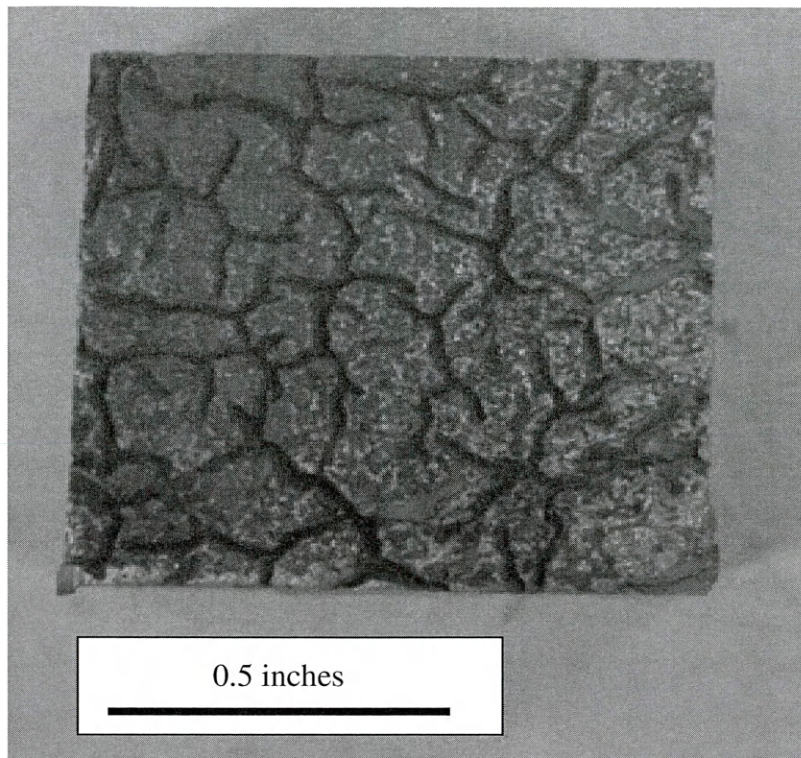
Figure 3.2 – Cracked boiler valve sample which corresponds to the Mikrosil[TM] cast shown in Figure 3.1.

Mikrosil[TM] cast clearly shows that the crack roots do not meet while the surface edges of the cracks appear to merge together. This observation seems to indicate that the cracks originated separately and grew into each other.

In addition to a network of independent singular cracks, some cracks have multiple branches. One such crack is shown in Figure 3.5. In these cases the areas where the cracks branch become wider and somewhat deeper than the crack segments that are strictly independent. Overall examination of the casts indicates that the majority of cracks intersect at the sample surface, however a relatively small fraction of them intersect at the crack root. The cracks do not appear to have a preferred orientation, which suggests that the flow of liquids or gases within the valve do not have a significant
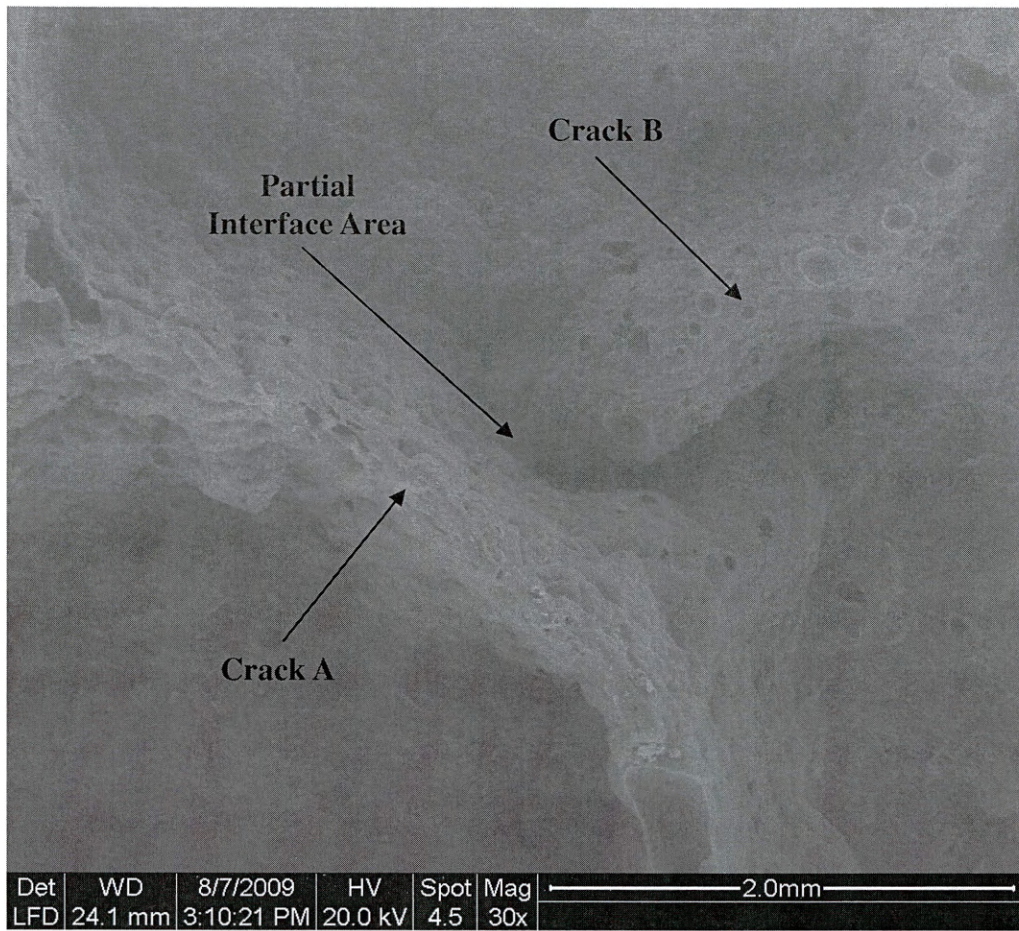
Figure 3.3 – SEM image of a Mikrosil^{TM} crack cast. Two cracks are shown with a partial interface existing between the cracks.
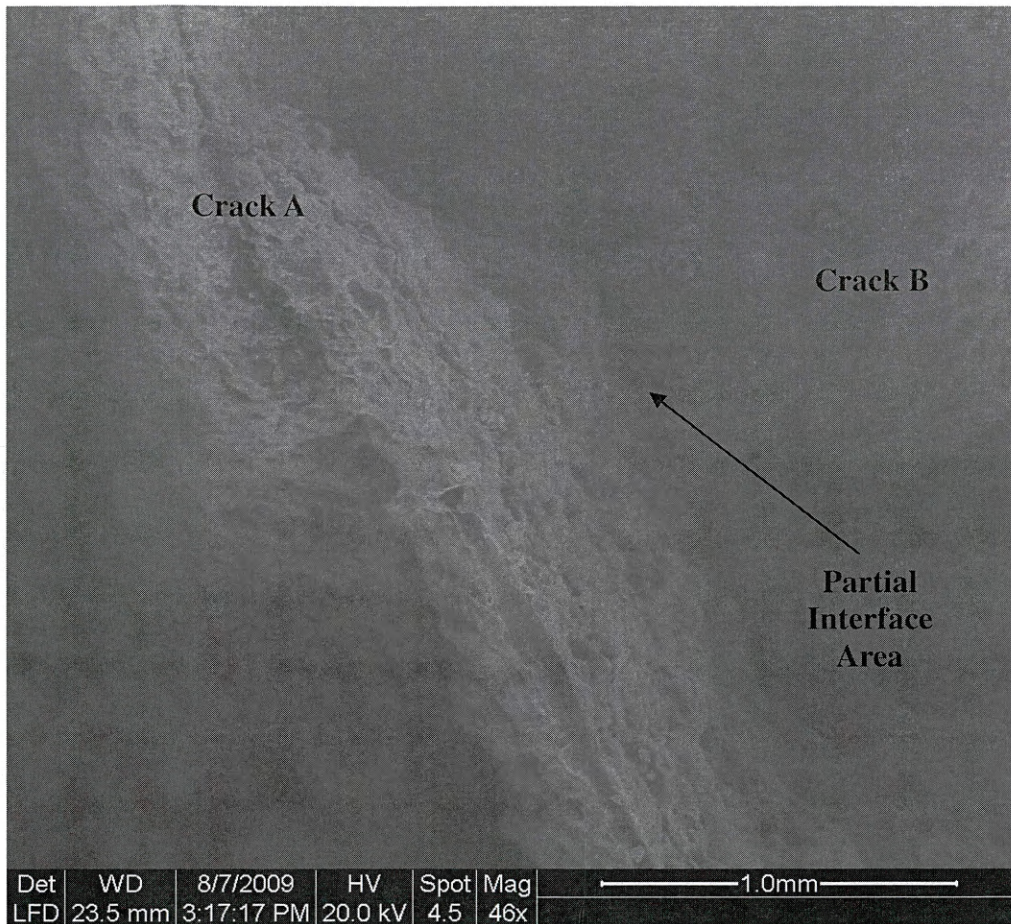
Figure 3.4 – SEM image of a Mikrosil™ crack cast. The cracks shown are the same cracks shown in Figure 3.3 at increased magnification and rotated slightly clockwise. Rough surfaces are those of resulting crack surfaces after cleaning and are not due to residual corrosion products within the cracks.

contribution to the formation mechanism. Due to the fact that a large number of widely spread cracks appear to have originated independently, it appears that the cause of the cracking is distributed across the entire interior surface of the boiler valves. This distribution suggests that a cause such as stress due to the internal operational pressure may have a role in the crack formation mechanism. If a material defect were the cause of the cracking, it would be expected that the cracks would start in a single location and radiate from there. In addition, because each crack has a heavy concentration of oxides present all the way to the crack root, corrosion is likely a contributing factor to cracking. Combining those two factors, stress corrosion cracking is likely the primary cause of cracking in these boiler valves. In stress corrosion cracking, the stress need not be sufficiently high to cause cracking on its own. Instead, the stress creates locations where material removal by corrosion is preferential. As these locations are corroded, greater stresses are concentrated at the resulting crack root, accelerating the corrosion and therefore the crack growth rate.

3.2 Filler Metal Development

Button melting was determined to be an effective method for filler metal production and was used for producing all alloy compositions tested. One limitation of the method is that a certain portion of the powders at the outer edges of the button melter cavity remained un-melted. It appears that the un-melted powder is displaced by the arc force and pushed to a location within the button melter where the arc cannot reach. These
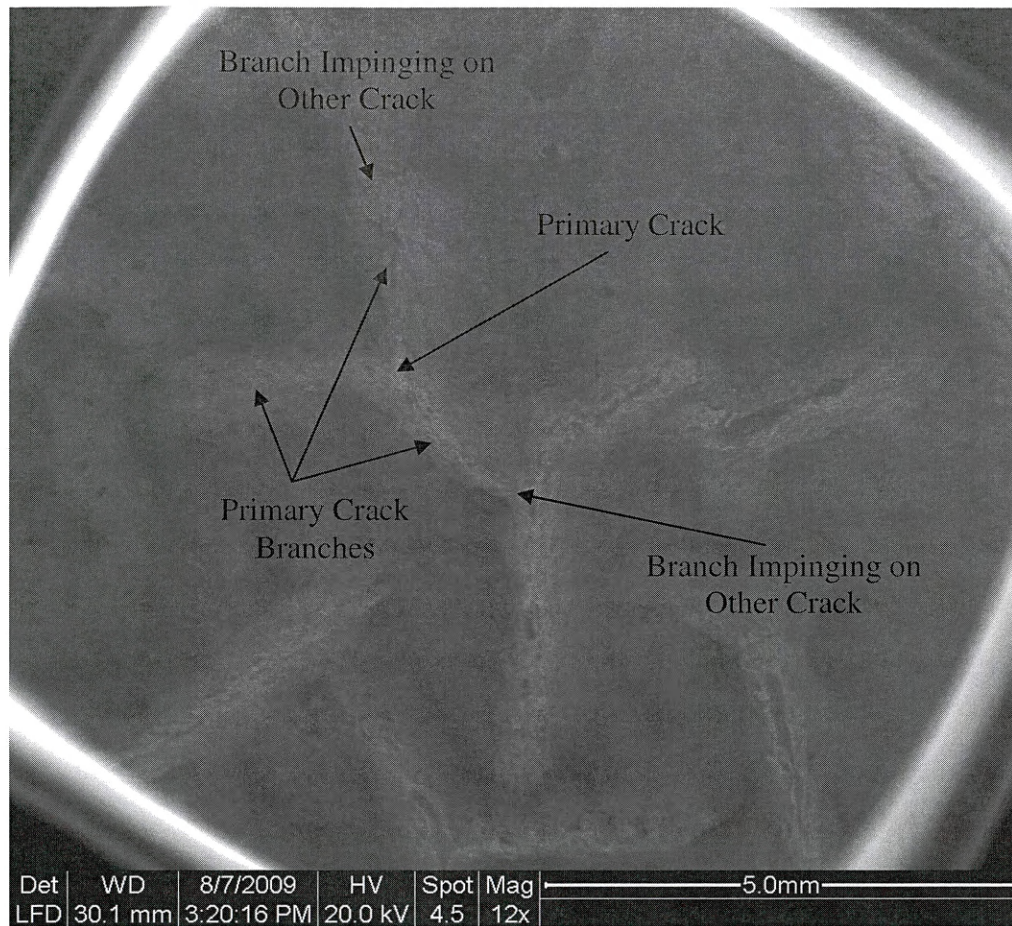
Figure 3.5 – SEM image of a Mikrosil™ crack cast. The primary crack system shown has three branches which all join together at a single point. In addition two of the branches impinge on other cracks in the same way as illustrated in Figures 3.3 and 3.4.

un-melted rims resulted in alloying losses in the final filler metal buttons. To account for the losses, each button was characterized using energy dispersive spectroscopy (EDS) to quantitatively determine their chemical composition data. For accuracy, all compositions reported are actual compositions as determined by EDS for the primary constituents. Compositions for phosphorus and carbon levels were assumed to be the target compositions because they were under the EDS detection threshold.

Results of sessile drop tests show clear behavior differences between the compositions selected. Tabulated results are shown in Table 3.1. The modified spreadability index is one of the properties used to characterize the ability of the molten alloy to flow on the steel surface. It is defined in Equation 3.1 where ΔA is the change in wetted area between the initial droplet and the droplet after spreading, Θ is the wetting angle, and m is the droplet mass. As shown in figured 3.6-3.8, sample G exhibited the best spreadability index, i.e. the largest ΔA and smallest wetting angle. Sample F ranked a distant second in terms of spreadability, but its wetting and spreading were still within an acceptable range.
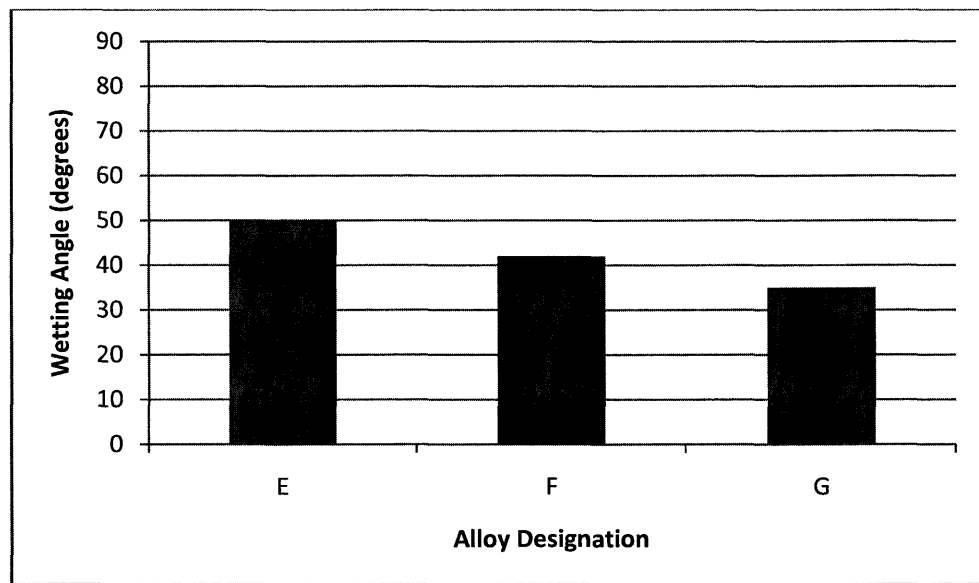
Figure 3.6 – Wetting angle for alloys E, F, and G. Alloy G exhibited the best wetting angle out of the three alloys shown.
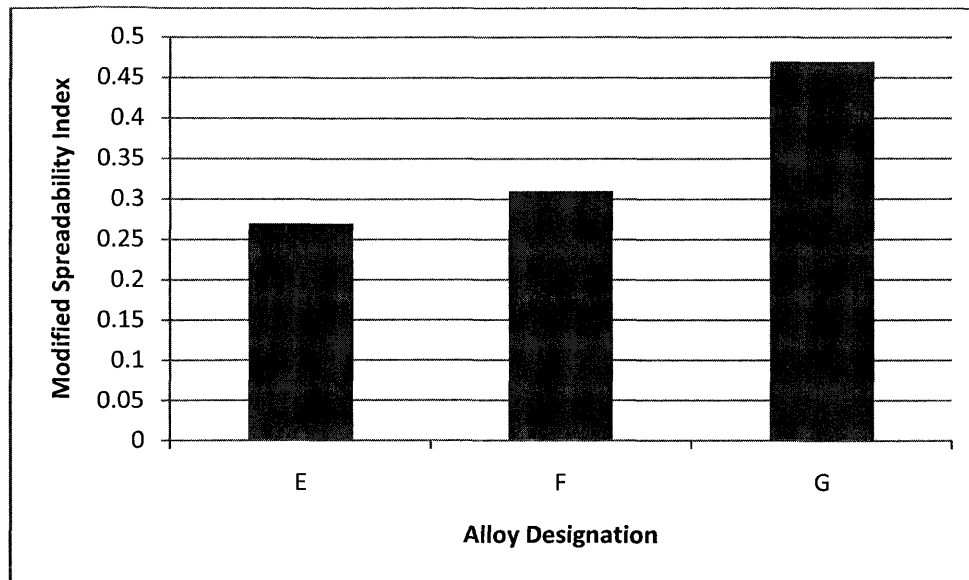
Figure 3.7 – Modified spreadability index for alloys E, F, and G. While alloy G showed the best spreading behavior, all three alloys were within an acceptable range.
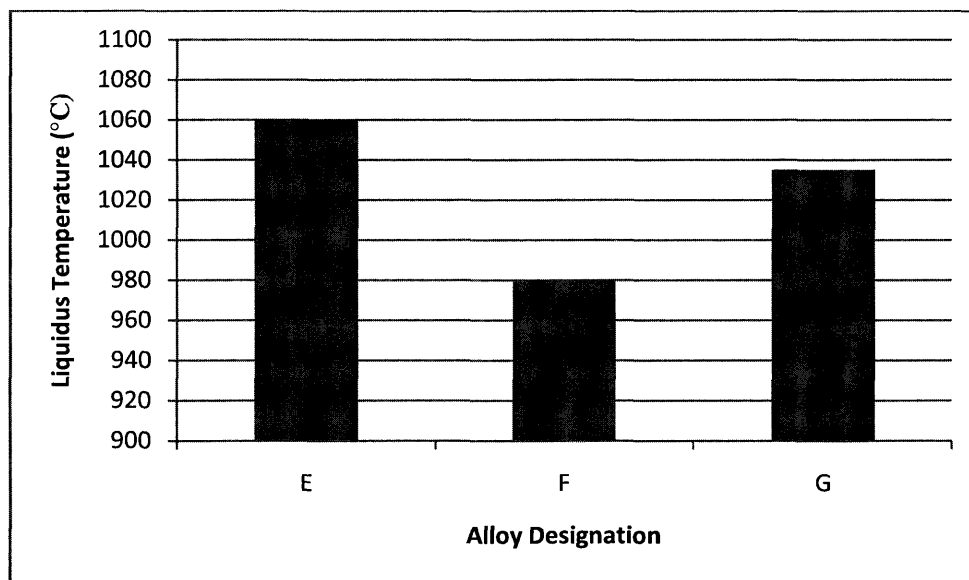
Figure 3.8 – Liquidus temperature for alloys E, F, and G. Alloy F exhibited the lowest melting point which figured strongly in the selection of the optimal alloy.

For selecting the candidate filler metal, other properties should also be considered.

As shown in earlier sections, melting temperature is a very important characteristic in

brazing filler metals. Samples B, C, and D did not perform well in this test, they did not

melt at the maximum furnace temperature of 1175°C. As such, these three samples were not considered as possible acceptable alloys for this application.

Additional characterization work was conducted on Alloy F using DSC to validate the observed properties as shown in Figure 3.9. The results confirmed that the solidus was near 935 C and that there were no significant phase changes present between solidification and room temperature that might otherwise cause unexpected behavior during brazing.
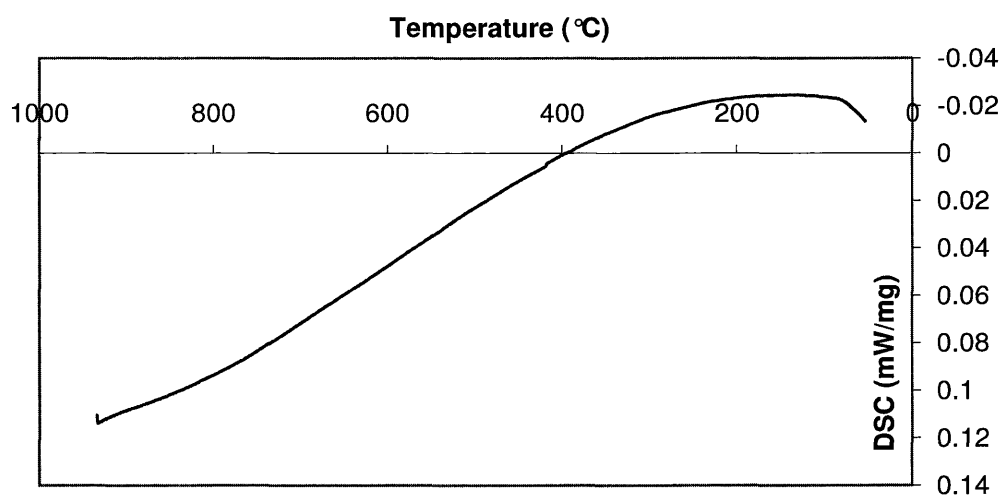
Figure 3.9 – DSC evaluation of alloy F illustrating lack of phase changes after solidification is complete.

Combining these results with the sessile drop testing (wetting and spreading), Alloy F was confirmed to be the best choice for this application with the best combined properties. Therefore, composition F was selected and is referred to as the custom filler metal alloy from this point on.

Table 3.1 – Results of sessile drop experiments performed on custom filler metal alloys. Composition balance is Nickel.

Property	B	C	D	E	F	G
wt% Si	12	11.7	29.1	10.5	14.1	11.5
wt% Cr	5	5	4	9.7	4.7	7.4
wt% C	0.08	0.08	0.06	0.06	0.08	0.08
wt% P	0.03	0.03	0.02	0.03	0.05	0.06
Wetting Angle (deg.)				50	42	35
Modified Spreadability Index				0.27	0.31	0.47
Tm (liquidus) (°C)	>1125	>1125	>1125	1060	980	1035
ΔTm (°C)				35	45	30

$$SI = \frac{\Delta A * \cos(\theta)}{m} \qquad (3.1)$$

3.3 Flow Analysis and Defect Formation

Once flow testing was complete, each experimental run was analyzed. The presence or absence of defects was recorded, along with their position within the joint as shown in Figure 3.10. The defects were examined individually to evaluate the mechanisms involved in their formation. In addition, the flow mechanism of the fluid within the joint was examined in detail.

During flow tests using the surrogate systems, two separate types of defects were observed. The most frequently observed defect was the formation of a fillet, which appears as a lack of fill at the joint edge opposite from where the filler liquid was introduced. It is referred to as a fillet-type defect because its physical appearance
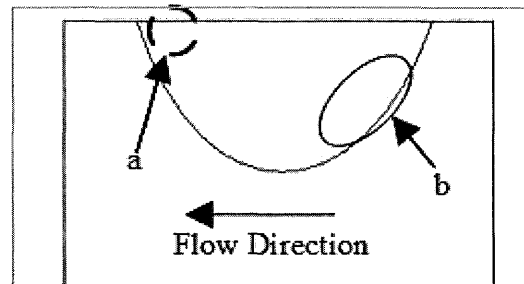
Figure 3.10 - Locations of Observed Defects
a- Fillet-type Defects
b- Pore-type Defects

resembles a fillet. This defect was only observed with shallow joints with a depth-to-width ratio less than 0.3, and could not be eliminated by introducing additional liquid to the joint or by vibrating the entire joint after filling. Liquid can be added in quantities greater than required to fill the joint. In these cases the filler liquid builds up on the inflow edge of the joint and does not eliminate the defect. The only way found to eliminate this defect type was to physically disturb the flow profile by providing additional liquid directly at the defect location and slightly overfilling the joint.

The mechanism for formation of fillet defects is consistent with surface tension-controlled flow. As the liquid fills to the top of the joint and the fluid flow stops, the liquid-solid contact angle is maintained with the bottom curved edge of the joint as shown in Figure 3.11. When the joint is relatively deep and narrow, surface wetting and the equilibrium contact angle causes the edge to reach the surface before the remainder of the fluid, allowing for the joint to fill completely. Figure 3.12 shows a deep crack configuration in which fillet-type defects are not observed. However, in shallow joints

the contact angle causes the bulk fluid to reach the surface on the feeding side before the edge fluid does. (Fig. 3.13) When this surface contact occurs, the surface energy forms an equilibrium contact angle. [13, 14]
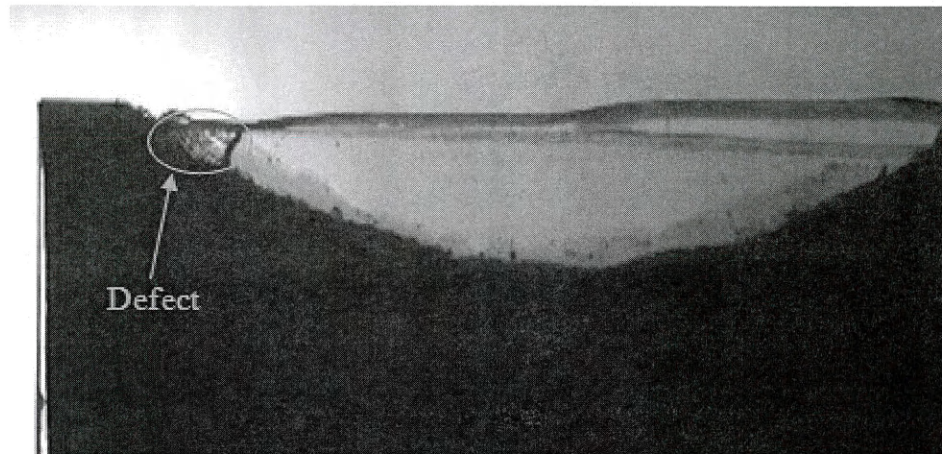
Figure 3.11 - Unfilled Joint End Illustrating Incomplete Filling at Terminal End of Flow Causing Fillet-Type Defect and Additional Filler Accumulating Above Top Surface of Joint
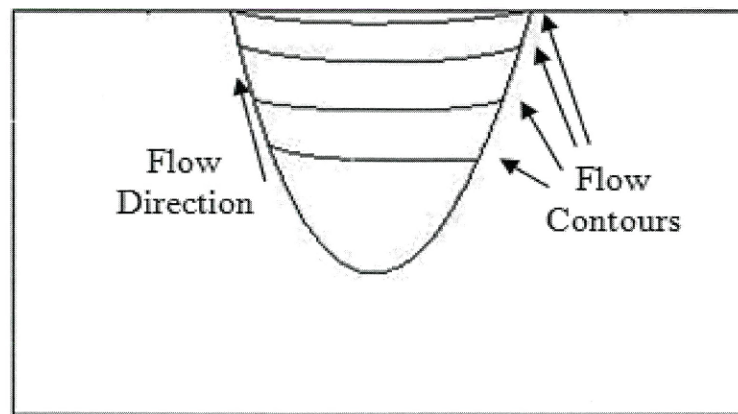
Figure 3.12 - Flow Contours Showing Flow Which Would Prevent Fillet Defect Formation
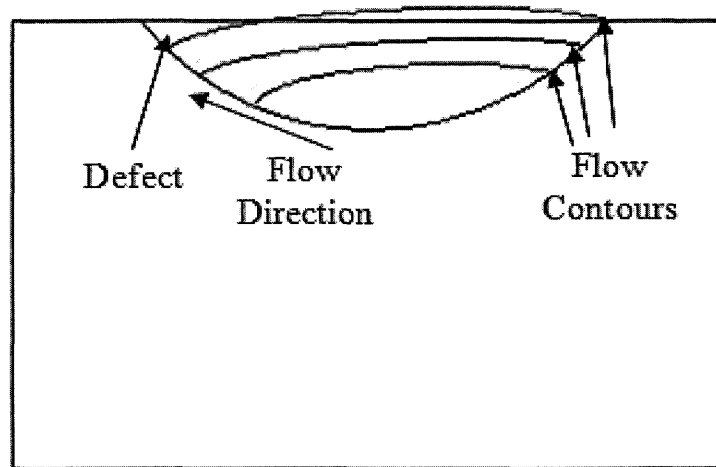
Figure 3.13 - Flow Contours Showing Flow Which Would Cause Fillet Defect Formation

This type of defect is evidence that surface energy still has a contribution to the flow and filling behavior of ultra-wide gap joints. If the surface energy contribution was near zero, the joint would fill to the surface without interruption. [15]

In addition, these fillet-type defects illustrate the significance of the narrow edge of the joint in flow behavior. During traditional brazing, the large planar surfaces dominate the flow of the filler metal due to the large surface area in contact between them and the filler metal. During ultra-wide gap brazing, on the other hand, the area of the joint edge surface (between the two faces) is large enough that it can also interact with the filler in a significant manner by forming an observable equilibrium contact angle large enough to influence the final filler metal morphology. This interaction allows the edge surface to influence the final geometry of the brazed joint. For instance, if the terminal end of the joint was in an inaccessible location, the defect would be preserved, creating a sharp stress riser which could lead to joint failure.

The second type of defect observed was a pore created within the joint itself. The location of the pore was consistently observed on the inward flow side of the joint, in contact with the curved edge. Once created, this type of defect could not be removed, and would only be detected in an actual brazed joint via non destructive or destructive testing after solidification was complete. Therefore, this defect type is of a greater concern when designing brazed joints.

Image analysis shows that the pore-type defects form during the initial flow of liquid to the bottom of the joint. As the liquid advances into the joint, any small disturbance to the liquid flow rate or path can initiate the formation of a pore. The disturbance can cause the transition from surface tension driven flow to pressure driven flow, which is required for defect formation. This observation gives some insight into the mechanism involved in the formation of the defect. Examining the fluid channel immediately before defect formation, good wetting exists on all sides of the flow as it advances, as occurs during traditional brazing [1]. However, as the defect begins to form, a wave of liquid forms and rolls ahead of the front, contacting the other face of the joint where the fluid had not yet wetted and trapping a small gas bubble underneath. Once the wave re-contacts the joint edge, the defect bubble becomes trapped and remains at a constant location through the remainder of the fluid flow. (Figure 3.14)

Observing the fluid edges in contact with the planar faces of the joint gives an indication of the reason for the formation of the pore-type defect. When the fluid face is

advancing slowly the fluid wets the surfaces well, advancing in a manner more consistent with traditional brazing.
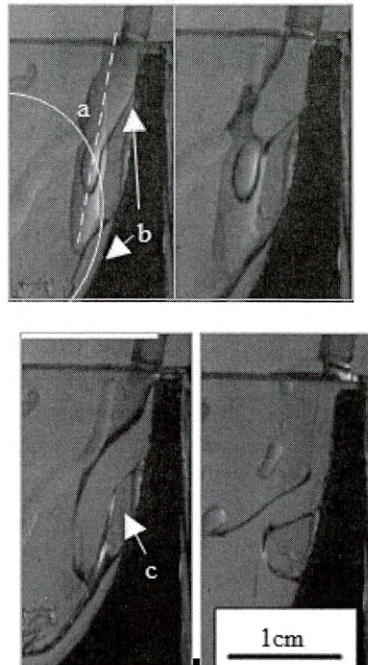
Figure 3.14 Formation of Edge Pore
a- Initial Fluid Flow to Bottom of Joint b- Joint Edge c- Pore Location

Once the fluid advances quicker, however, there is a larger volume of liquid than can be contained by the existing stable channel. The fluid then folds over the existing channel boundaries and the advancing front moves past the wetted edge. As it progresses it collapses back into contact with the walls in a cyclic manner, re-establishing the expected wetting behavior momentarily as illustrated in Figures 3.15 and 3.16.

In Figure 3.15 the relative height of the top meniscus of the fluid is graphed with respect to time. The height is normalized by the maximum meniscus dimension

measured during the flow trials. The measurement location is illustrated on Figure 3.16. The wetting cycles from good wetting to poor wetting and then back to good wetting. Representative frames, shown as A, B, C, and D, from which data was extracted are shown in Figure 3.16.

In frame A, the fillet is clear and of equilibrium magnitude. As time progresses, frame B shows the fillet shrinking as the volume of flow begins to overcome the surface tension control mechanism. When the fillet becomes convex as seen in frame C, appearing lighter than the background instead of darker, the pressure-driven flow component becomes dominant, eventually leading to frame D, where the concave fillet is re-established as shown by the return of the dark colored fillet and normal flow resumes. The color of the fillet is caused by optical refraction of light passing through the curved surface. When positive wetting is present, light trying to pass through the fillet is redirected, causing a dark colored interface. However, when the wetting is negative, the light is able to pass through without diversion, causing the interface to take on a white color.

Non-wetting advance, also known as pressure driven flow does not always create a defect within the joint. The majority of the time, the advancing wave collapses back onto the same wall which it originated from as a result of decreasing flow rate, widening the fluid channel without creating a defect. When this collapse occurs, good wetting is re-established along the entire interface, allowing normal quality adhesion to occur upon
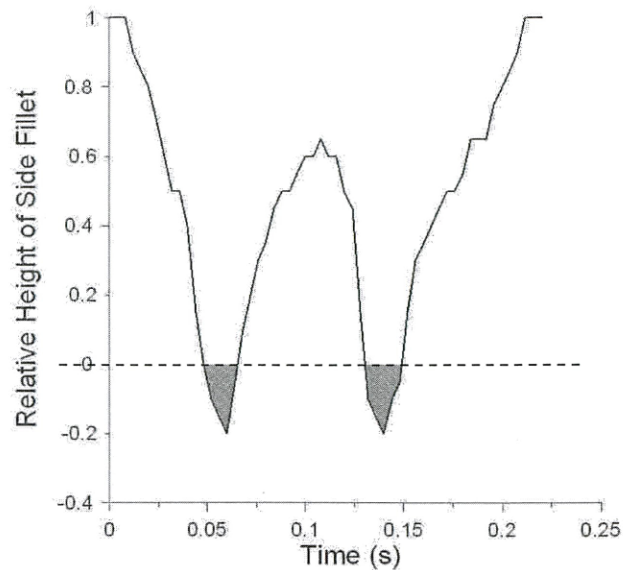
Figure 3.15 Variation of Meniscus Height with Time as Measured at Dotted Line on Figure 3.16, Grey Areas Indicate $\theta > 90°$ Showing Pressure-driven Flow
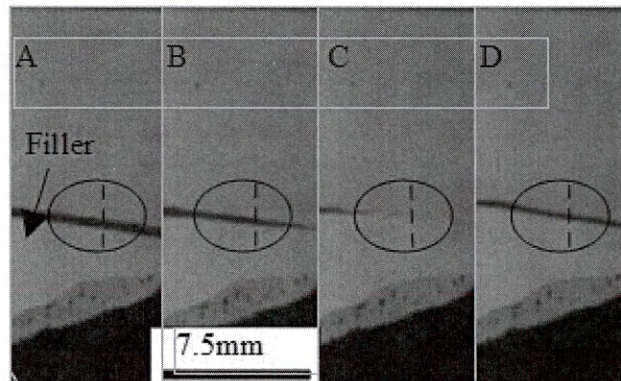
Figure 3.16 - Detail of Flow Images Illustrating Changes in Wetting Behavior as a Function of Time. Orientation is Identical to Figure 3.9.

solidification. Non-wetting flow can also occur when the fluid is already in contact with both planar walls. This type of flow is most easily observed near the leading edge of the flow as the fluid fills the joint from the bottom.   In this region there is a gradient in the speed of advance, illustrating the dynamic equilibrium point between wetting driven and pressure-driven flow. (Fig. 3.17) In the slower moving right hand region, wetting driven

flow exists, while in the faster moving left hand region pressure driven flow exists. The transition point between the regions is moving at the transition velocity.

Observing the formation mechanisms for both types of defects, along with other flow patterns within the joint, it can be seen that neither surface tension-controlled flow or pressure-controlled flow are entirely dominant during the flow process. Instead, the control mechanism changes dynamically with changes in the fluid flow rate. This phenomenon is significant to crack repair because in the field it is predicted that the repair procedure will be carried out using manual oxy-gas brazing. In this situation the technician performing the repair has significant amounts of control over the speed at which the filler metal is added to the crack. Therefore, the technician has a certain amount of control over the flow mechanism which exists and thereby the likelihood of flow defects occurring. If the filler metal is added relatively quickly then there is a higher likelihood of defects occurring, however slower filler metal additions decrease the chance of defects being produced. Control of the flow rate can be achieved by increasing or decreasing the rate at which filler metal rod is added by the welder. This control is particularly significant because in crack repair scenarios the ability to inspect the joint for flow defects after brazing may be limited. Filler metal cannot be added from multiple locations in the crack network during a repair step unless care is taken to prevent the creation of added defects.

3.4 Crack Preparation

Initial joint cleaning testing determined that the hydrogen peroxide was effective at removing particulate oxides from within the cracks themselves. In this situation the
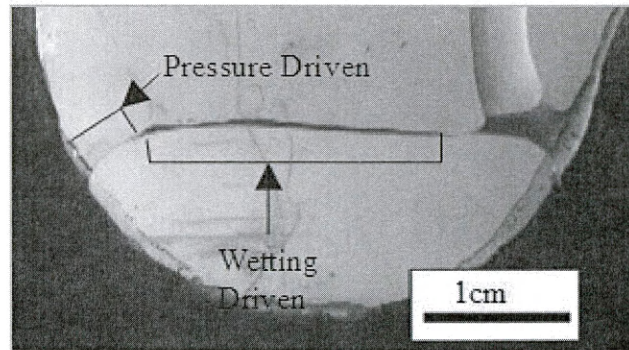
Figure 3.17 - Detail Illustrating Pressure-driven Flow and Wetting Driven Flow Regions

hydrogen peroxide caused gaseous oxygen bubbles to nucleate on oxide particles. The bubbles then detached from the cracks and floated to the surface, taking the loose oxide particles with them. It should be noted that extended immersion in hydrogen peroxide is not suggested, given that hydrogen peroxide is a strong oxidizing agent and can quickly increase the total oxide thickness on the surface being cleaned.

Use of the DTPA based cleaning solution presented more challenges to successful cleaning. Original specified procedures from the EPRI crack cleaning document [2] indicated that the cleaning should be carried out at room temperature. When testing this section of the procedure, it was quickly observed that while the solution did have success at removing oxides from the cracked surfaces, the rate of removal was very slow. To clean a single surface, over one week of continuous immersion was required. This cleaning was carried out until there were no visible oxides on the surface or within the cracks. It was obvious that more rapid cleaning was required for the cleaning procedure to be successful.

Possible causes for slow cleaning were determined to be slow chemical kinetics as well as low DTPA concentration. Both causes have a common possible solution. Increasing the cleaning temperature increases chemical kinetics substantially. In addition, DTPA has increasing solubility in water as the temperature increases. These factors led to the decision of conducting the cleaning experiments at a higher temperature. Approximately 80 $^{\circ}$C was selected as the cleaning temperature to strike a balance between process speed and safety. The temperature was below the boiling temperature of the solution, so little release of hazardous materials to the surrounding environment is expected. The safety margin of at least 20 $^{\circ}$C should be sufficient to prevent accidental boiling in both laboratory and industrial conditions.

When tested at 80 $^{\circ}$C, chemical cleaning was accomplished far more quickly, with immersion times of approximately 24 hours, one seventh of the time required at room temperature. Using this technique, it was possible to remove all visible oxides from both the top surface as well as the cracks themselves.

After the oxides were removed, the cracked surfaces were then rinsed using a dilute citric acid solution to remove any residual cleaning solution and other contaminants followed by a distilled water rinse and immediate drying using compressed air. It should be noted that the cleaned surfaces become sufficiently clean that they become readily susceptible to atmospheric corrosion. Because of this time sensitive behavior, cleaned surfaces should either be brazed immediately or stored in a desiccator

system. In the industrial repair situation, brazing should follow the cleaning steps as soon as the surface is dried.

3.5 Brazing Repairs

Once cleaning is completed, cracked surfaces are ready to be brazed. The first brazing trial used AWS alloy BAg-22 (49Ag 16Cu 23Zn 4.5Ni 7.5Mn), which is referred to from this point as the silver-based filler metal. This alloy was selected due to its high chromium content, which is desirable because it will enhance the service performance of the repaired brazed joint in the boiler environment and resist further corrosion. A sample of this alloy was placed on the surface of the cracked samples. Because it was obtained as a wire, the filler metal was wound into a tight bundle to facilitate melting and consolidation. During this trial no fluxes were used and the sample was furnace brazed using the same furnace setup as the sessile drop tests. When brazing was complete surface examination of the sample suggested very little flow of the filler metal. While the filler metal had consolidated in some areas, it appeared that complete melting had not been achieved. The filler metal retained a shape close to that of the original wire bundle and did not flow beyond its original footprint.

After sectioning the sample as shown in Figure 3.18, examination confirmed the assessment made at the initial visual examination. While the filler metal did form a metallurgical bond in limited areas under the initial footprint, meaningful filler metal flow did not exist. In addition, sections of the consolidated areas showed visual evidence of the individual wires in the bundle. These observations suggest that the filler metal did

not completely melt even in the areas which appeared to have flow. In addition, many of the wires did not melt or flow at all and showed only evidence of some softening. Finally, the filler metal was also confined to the surface, showing no flow into the cracks themselves.

The second test performed used the custom designed filler metal alloy. It was decided that the alloy should be applied in paste form to allow for better flow into the cracks. A small amount of petroleum jelly was used to bind the filler metal powder together. For this test a two hour hold time was used at temperature. These longer brazing times were intended to allow the filler metal sufficient time to consolidate since it was not pre-melted. Examination of the sample after brazing showed particulate flow deep into the cracks shown in Figure 3.19. Filler metal particles were clearly evident at all locations within the cracks as well as on the surface.
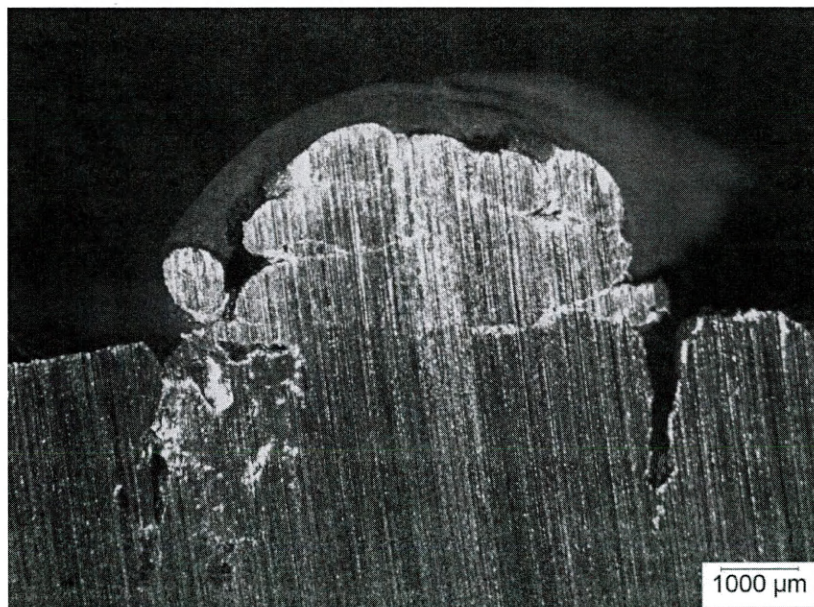
Figure 3.18 – Cross section of initial braze test using silver-based filler metal. Filler metal remains confined to its initial morphology on the surface of the sample.

However, these particles did not consolidate into a solid filler metal. Some sintering was present which allowed for the filler metal particles to adhere to each other as well as to the cracked surface. The adhesion was significant enough to prevent easy manual separation of the particles. However the interaction was insufficient to provide consolidation between the particles.
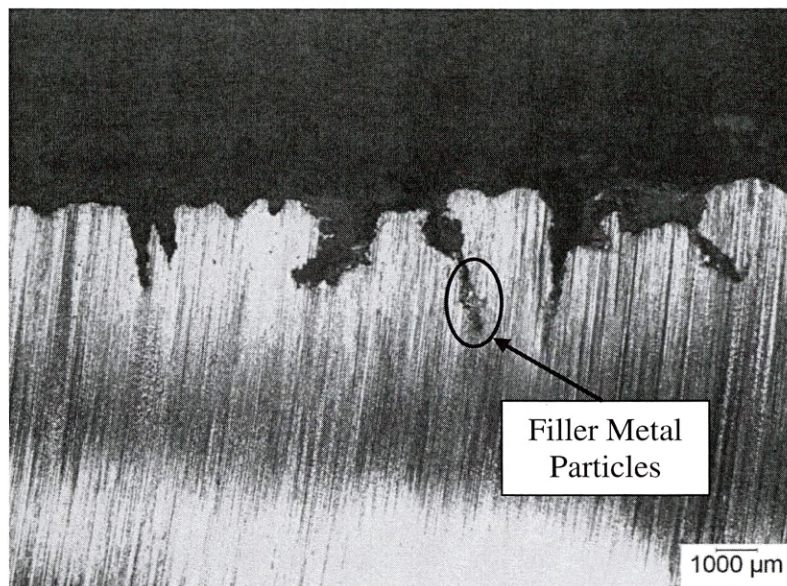
Figure 3.19 – Initial brazing test using nickel-based filler metal. Particles of filler metal are present within cracks but are not consolidated.

To alleviate the issues discovered in the first two tests several procedural changes were implemented. In all further tests, the filler metal was pre-melted into consolidated buttons before brazing. In addition, a potassium fluoride based commercial brazing flux was used to further reduce oxidation and encourage filler metal flow. The flux was applied to both the filler metal and base metal in order to allow for maximum oxide dissolution. The flux was manually worked into the cracks, however it did not reach the crack roots during initial application. The extent of the initial flux penetration was not

predicted to significantly influence the cleaning behavior because during the brazing cycle the flux became more fluid and exhibited flow to the crack roots.

A third test was conducted using these changes applied to the silver-based filler metal. Because the filler metal was pre-melted into a button, its placement was localized to a small portion of the cracked surface. When completed, the brazed surface showed substantial improvement. The filler metal melted completely and showed flow throughout the network of cracks. In addition, the filler metal exhibited flow to areas remote to its original position on the surface. For experimental trials 5 grams of filler metal were used for each 1 square inch sample. The amount of filler metal required is a function of the depth and width of cracks present and must be evaluated based on the Mikrosil™ casts. Sections of the sample showed flow deep within the cracks at all points on the sample. The high fluidity of the filler metal did, however, exhibit some problems, e.g. a substantial portion of the filler metal flowed off the edge of the sample. Consequently, there were areas at the top of the cracks that were not filled, as shown in Figure 3.20. Wetting of the edges of these areas indicated that they were filled at one point during the brazing process but were then subsequently emptied as the filler metal flow continued to a greater extent. This phenomenon is detailed visually in Figures 3.21 and 3.22.

While the filler metal did flow deep within the cracks, in some cases it did not reach all of the way to the crack root. In all cases where the root was not filled a dark colored granular substance was observed filling the remainder of the crack root as
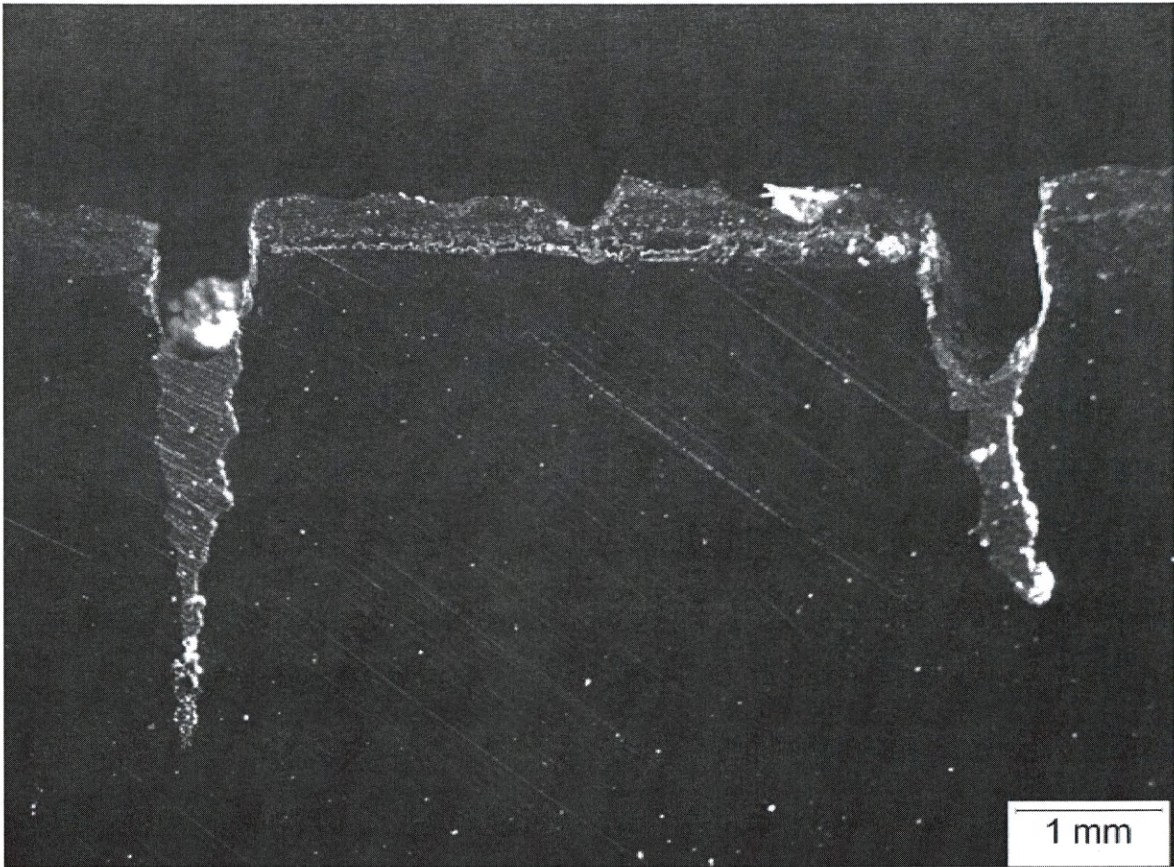
Figure 3.20 – Stereo optical image of brazed crack showing extent of flow as well as emptying at crack mouth.
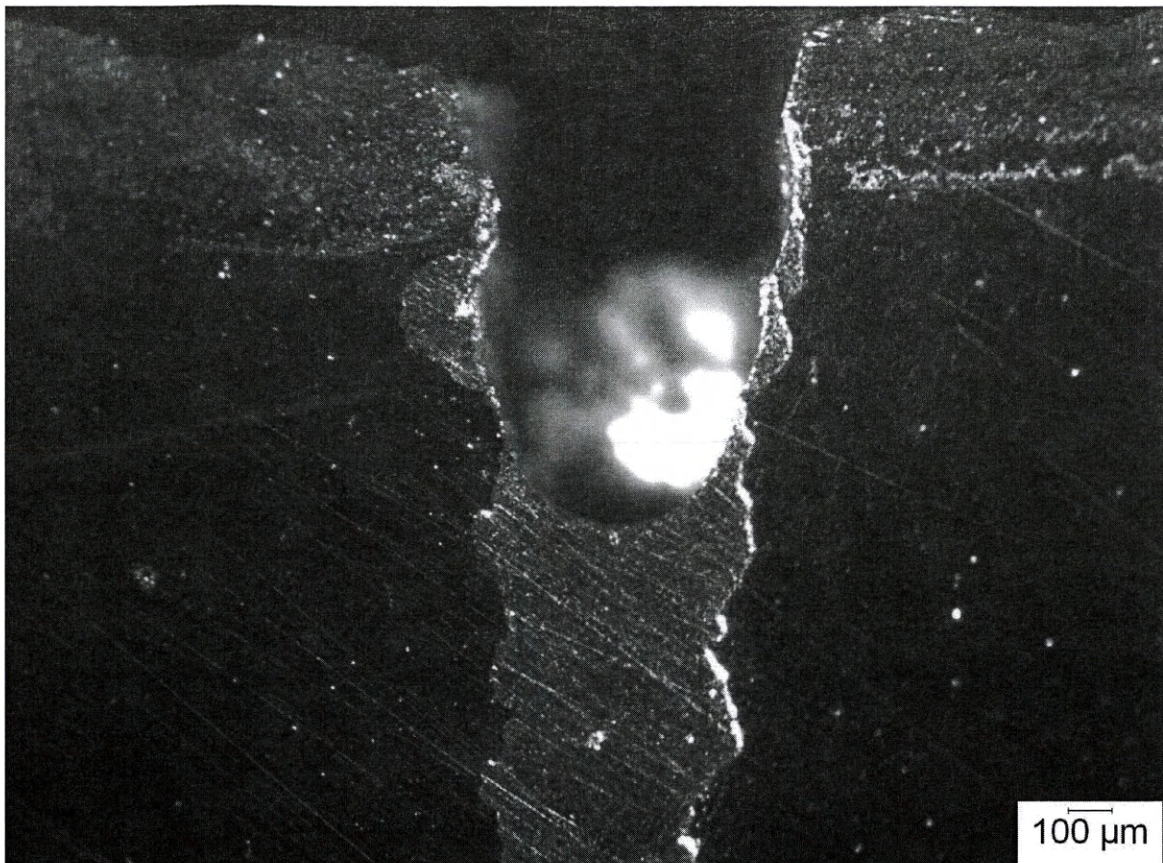
Figure 3.21 – Stereo optical image of brazed crack mouth. Filler metal layer is evident along crack edge illustrating the existence of filling and subsequent partial emptying of the crack.

Figure 3.22 – Micrograph of brazed crack mouth. Remaining filler metal after partial emptying is evident in surface roughness on the crack surface.

illustrated in Figure 3.23. SEM analysis identified this substance as a mix of iron oxides as well as a layer of brazing flux separating the filler metal and the iron oxides. The layer of flux was crystalline in surface appearance and exhibited some voids that had a crystalline appearance which can be seen in Figure 3.24. From the presence of these deposits it was determined that the cleaning procedure, while effective, was not able to remove 100 percent of the oxides from the cracks, particularly in the crack roots. The deepest cracks were more likely to exhibit this incomplete filling suggesting that the cleaning effectiveness is linked to crack depth and morphology.
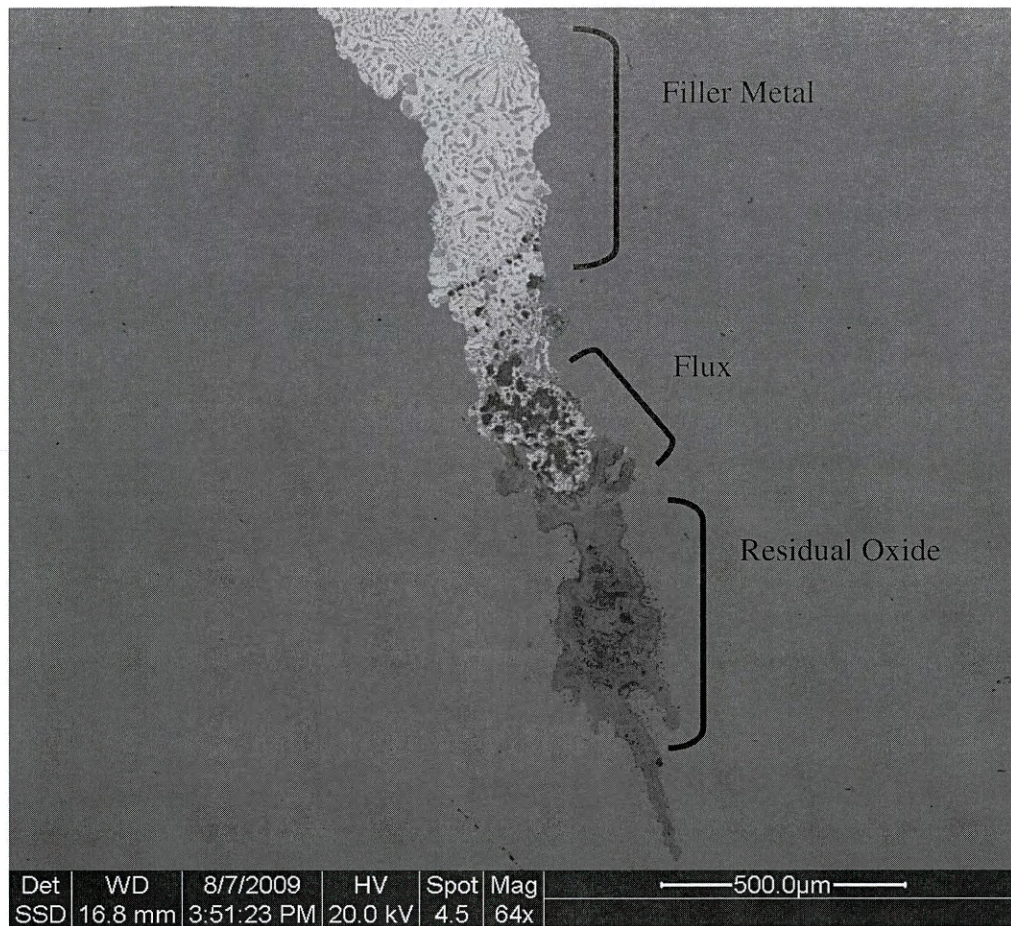
Figure 3.23 – Backscatter SEM image of crack root showing residual flux layer and oxide deposits.
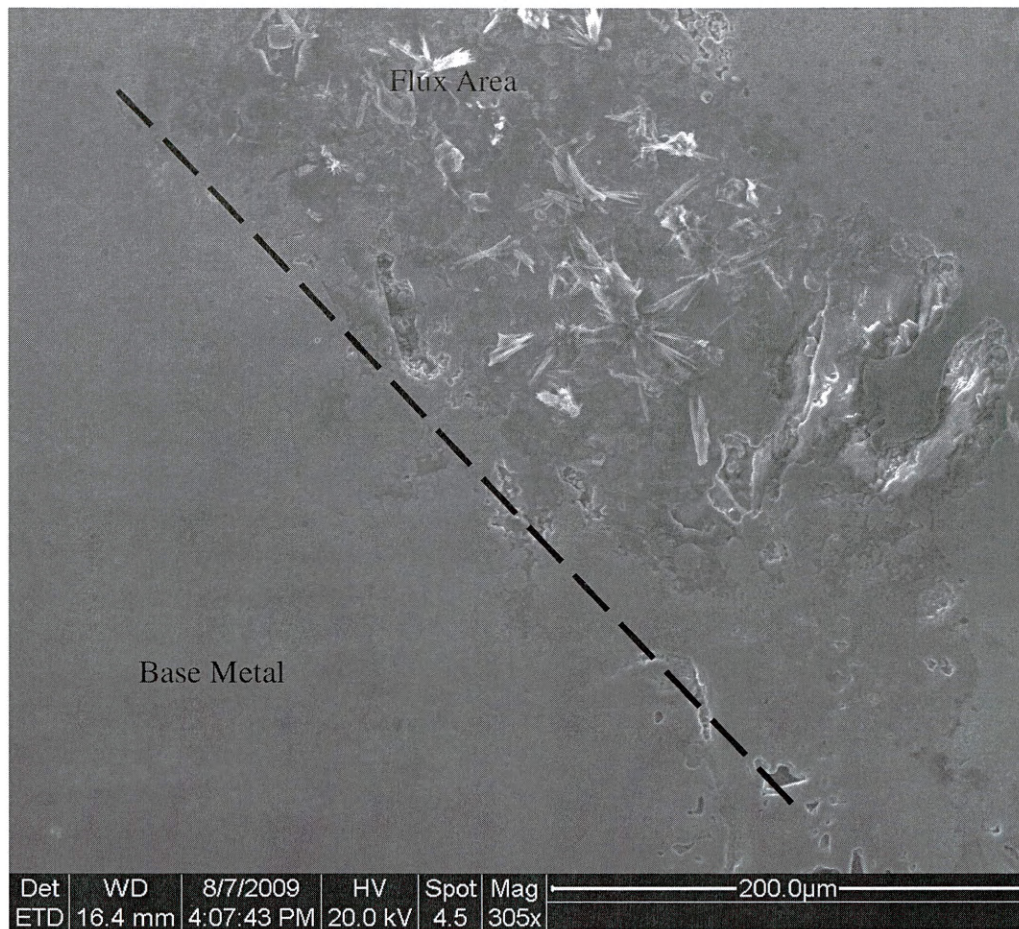
Figure 3.24 – Secondary electron SEM image showing the physical morphology of the residual flux in crack root.

Two methods were then implemented to reduce the impact of these remaining defects. The time used for crack cleaning was increased by an additional six hours to remove a greater amount of oxides at the crack root. In order to prevent flow off the surface of the samples a GTAW bead was run along the outer edges of the samples with the intention of mechanically confining the filler metal.

After applying these methods to sample 4, both the overflow problem and the remaining oxide in crack tips were improved substantially. The GTAW bead was

successful at eliminating overflow from the sample and it allowed the cracks to remain filled to the surface. Although the top surface was not smooth, the remaining roughness did not appear to present any substantial defects of concern. In addition, the more extensive cleaning allowed for a greater proportion of cracks to be completely cleaned and filled and reduced the volume of oxide in the remaining cracks.

The sections were then examined using both optical and electron microscopy for the presence of defects. It was determined that in cracks which filled completely, defects were rare. In eight deep cracks that were examined only one defect was observed which is shown in Figure 3.25. The defect appears to be caused by a small residual oxide particle trapped by surface roughness of the crack surface. This defect was a small round pore measuring approximately 30 microns across. All other areas of these cracks exhibited complete wetting across the entire interface area as shown in Figure 3.26. In addition, no intermetallic compounds were detected at the interface. The absence of intermetallic compounds is an indication of a high strength interface between the filler metal and base metal. Neither one of the two filler metals resulted in intermetallic compound formation during brazing.

In cracks which had residual oxide deposits at the root, a greater concentration of defects was observed. These defects were limited to the areas of the crack near the residual oxide deposit. All discontinuities were observed in these areas and consisted of inclusions of oxide or flux trapped within the filler metal.
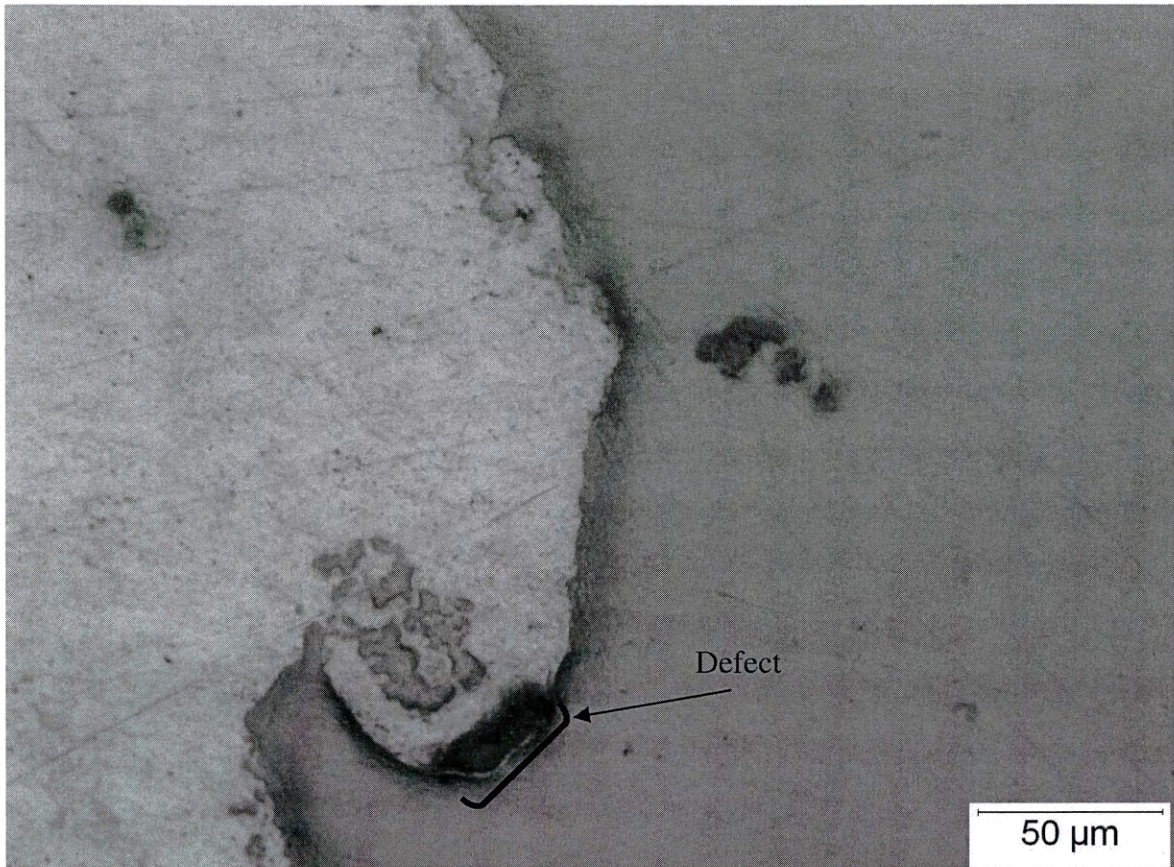
Figure 3.25 – Micrograph of brazed crack with discontinuity present. Discontinuity appears to be residual oxide trapped at the crack surface.
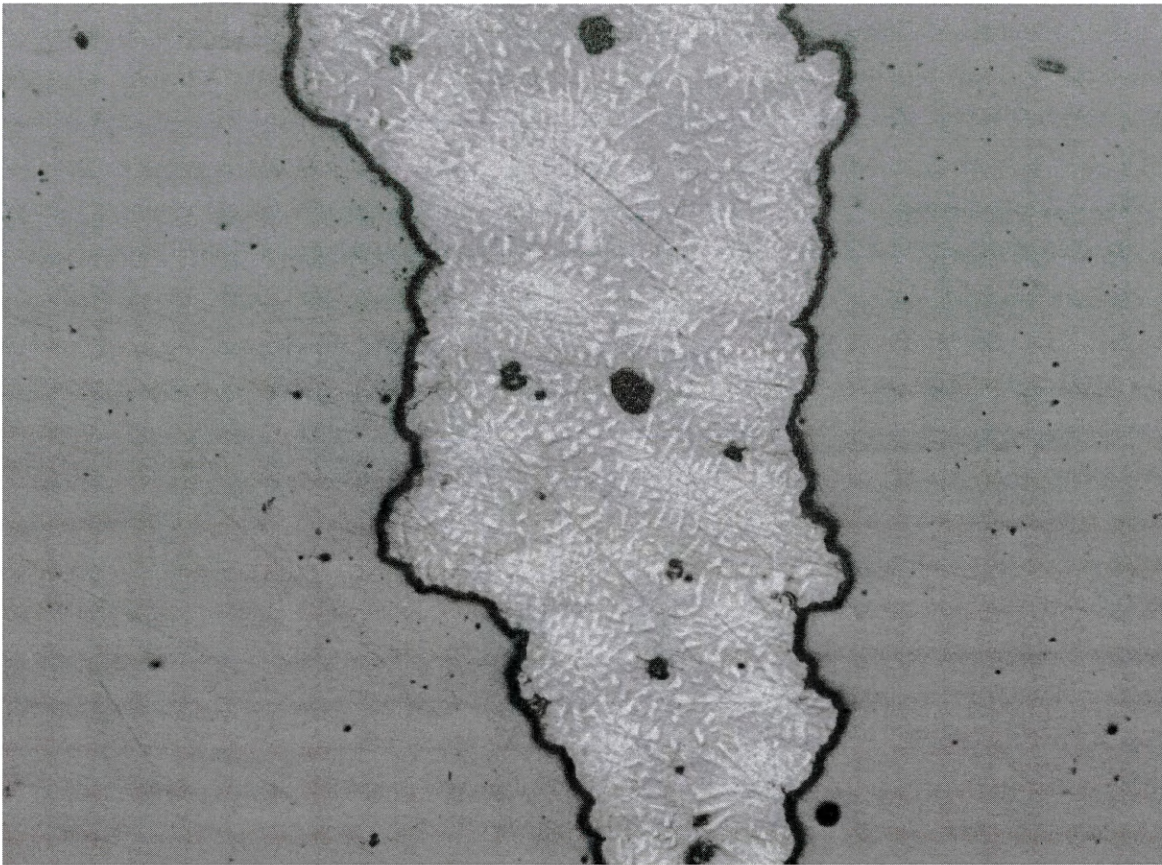
Figure 3.26 – Micrograph of brazed interface after polishing with no etch. Wetted interface is continuous with no porosity or discontinuities. Dark particles indicate areas preferentially etched in filler metal.

64
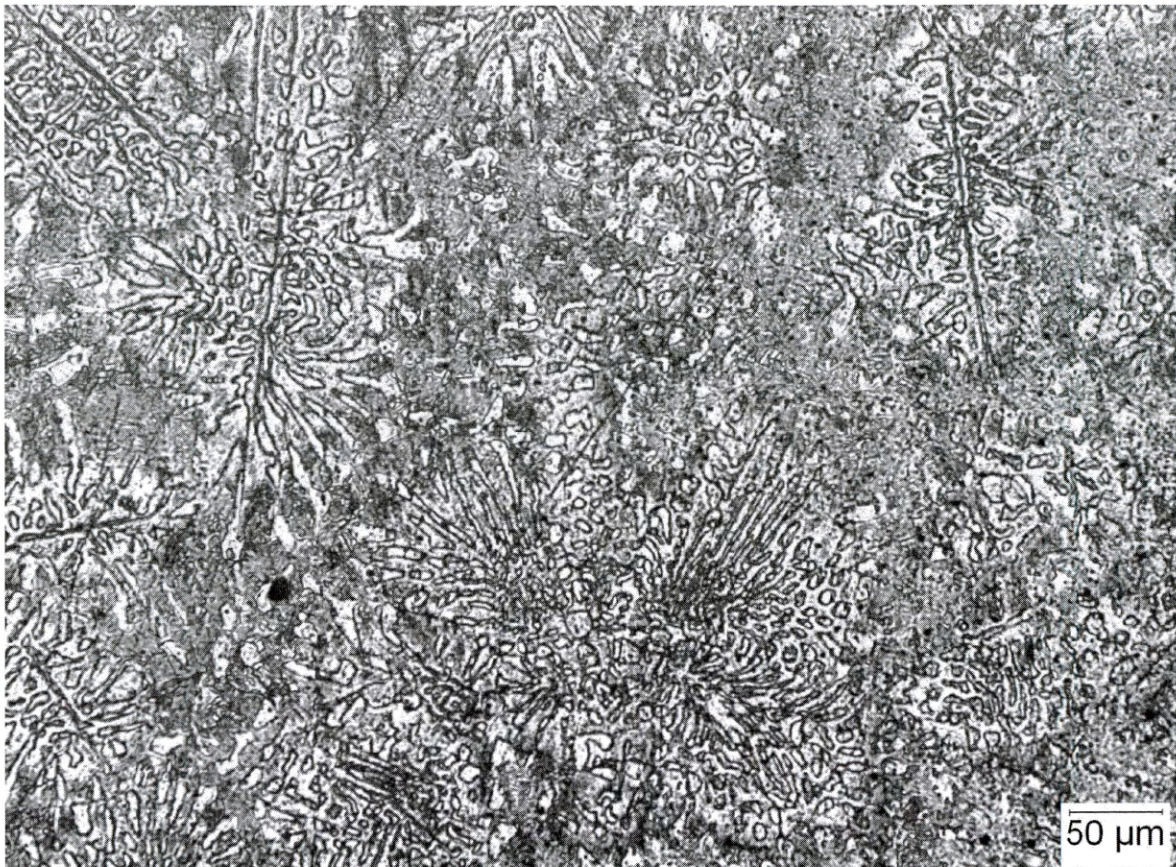
Figure 3.27 – Micrograph of silver based filler metal braze. Hydrogen peroxide / ammonium hydroxide etchant.

Polished samples were etched using a solution of 50% concentrated hydrogen peroxide and 50% ammonium hydroxide. The microstructure revealed a dendritic solidification structure as shown in Figure) 3.27.

The dendrites appear to form as colonies which are evenly distributed within the filler metal area. There does not appear to be any preferential orientation for the dendrite colonies, which indicates that there is no strong thermal gradient present during solidification which would normally produce a preferential solidification orientation.

This phenomenon is consistent with the processing parameters of the samples. Furnace cooling provides very small thermal gradients within the parts.

In addition to the orientation of the dendrite colonies, their internal structure indicates a fairly uniform thermal profile. The dendrites themselves form in all directions from the nucleation site of the colony as shown in Figure 3.28.
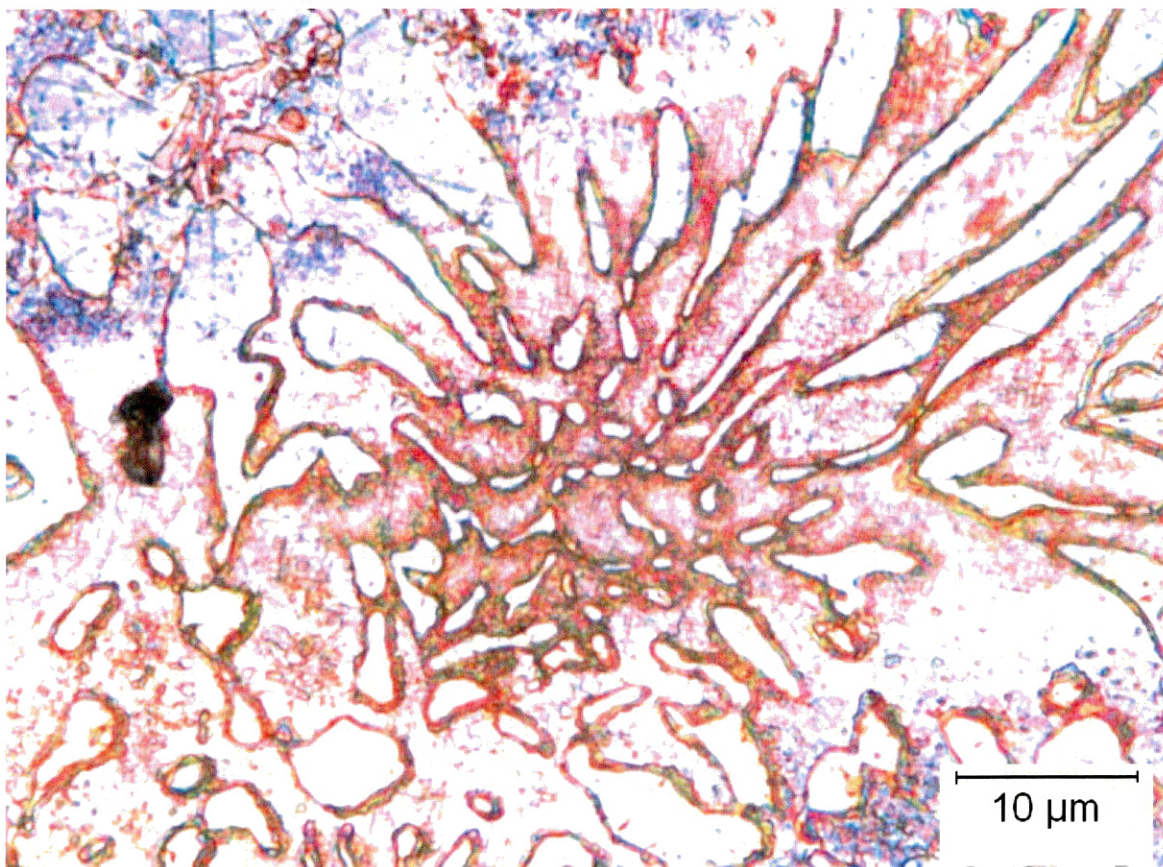
Figure 3.28 – Micrograph of silver based filler metal illustrating one dendrite colony.

One additional property of the brazed cracks which is of concern is their ability to survive subsequent cleanings. This chemical resistance is significant because a cracked

boiler component may require multiple repairs over the course of its lifetime. To evaluate

the repair behavior in this situation a sample of brazed material was exposed to the oxide

removal cleaning procedure. It was determined that the cleaning process did

preferentially remove filler metal instead of base metal. The rate of this preferential

removal was approximately 1mm of filler metal removal over a complete cleaning cycle.

The preferential removal rate was low enough however that the repair would not be

completely removed and the filler metal would still remain within the bulk of the repaired

cracks.

3.6 Repair Procedure

Taking into account the entire group of steps required in order to create a quality

repair, it is important to bring those steps together in a single location. Below is the most

successful repair process determined from experimental work.

When a crack is discovered it must first be characterized to determine the need for

repair. Phased array ultrasound testing should be used to measure the dimensions of the

crack so that a determination can be made. Assuming that the crack is determined to be

large enough to require repair (as defined by EPRI failure analysis standards), the crack

as well as the surrounding surface should be cleaned.

The crack area should first be mechanically cleaned using a wire brush or other

similar tool. Compressed air should then be used to remove any remaining loose oxide

particles. The area should then be mechanically isolated for chemical cleaning. If the

entire valve is cleaned, a significant amount of cleaning solution will be required. In order to limit repair costs, portions of the valve not being repaired should not be cleaned.

The first chemical cleaning step should be a hydrogen peroxide bath lasting no longer than five minutes. A hydrogen peroxide solution of concentration not greater than three percent should be introduced into the crack area. As the hydrogen peroxide decomposes, loose oxide particles will adhere to the bubbles and float to the surface of the solution. After the hydrogen peroxide is removed, the cracked area should be immediately rinsed using water. De-ionized water was used for all cleaning steps during laboratory trials. The purity of water used in the field must be evaluated for each individual step.

The second chemical cleaning step is immersion in the DTPA cleaning solution detailed in the experimental procedure section. The solution should be heated to a temperature between 60 and 80 degrees Celsius. This temperature should be maintained for the duration of this step, approximately 30 hours. The chemical cleaning solution should be changed when it becomes visually opaque and will have to be changed several times during the cleaning process. One alternative to changing the solution periodically is to continuously circulate the cleaning solution from an outside reservoir. The solution must still be monitored to detect if the color changes and the solution becomes opaque. The used cleaning solution should be disposed of according to local hazardous materials regulations. The DTPA cleaning step should be continued until the cleaning solution no longer changes color after 30 minutes of contact without circulation, even if this requires

longer cleaning than the specified 30 hours. In addition, the cracked area should be visually examined to ensure that all oxides have been removed.

Immediately after the DTPA step is completed the cracked area should be rinsed using room temperature citric acid to remove any residue and distilled water to complete the cleaning. This rinse should be followed by thoroughly drying the cracked area to prevent re-oxidation of the clean surface.

The crack should be brazed immediately after cleaning. The allowable hold time is a function of current humidity, but should be minimized in all cases. Potassium fluoride based brazing flux should be applied liberally to the cracked area before heating. The cracked area should then be heated to brazing temperature as rapidly as possible without local melting of the steel. Heating should be accomplished using an oxy-gas torch system and should be localized as much as possible to the area being repaired. Brazing must be accomplished in the flat position. If the cracked area is out-of-position, the valve must be manually rotated to bring the crack into the flat position. The filler metal should then be added to the primary crack area until the entire heated area is filled. Filler metal should be added at a relatively slow rate to minimize the possibility of flow defect formation. The filler metal will not flow into areas which are cooler than the melting temperature of the filler metal, therefore local heating can be used to restrict the flow of the filler metal. After the filler metal has reached the desired areas, the heat should be removed and the filler metal should be allowed to solidify.

No post-braze heat treatment is predicted to be required, however the resulting braze should be inspected using phased array ultrasonic testing to verify satisfactory joint penetration and repair quality.

Out of position cracks are currently not easily brazed using this technique. Therefore, it is important that the valve be positioned so that the cracked area being repaired is in flat position. A summary of repair procedures is included in appendix A.

3.7 Limitations of Ultra Wide Gap Brazing

Ultra wide gap crack repairs have a sufficient volume of filler metal such that the mechanical properties of the filler metal create the majority of the joint strength. Due to the fact that many filler metal alloys such as silver based alloys have much lower mechanical strength than the base metal (low alloy cast steel) the repaired locations have the potential to become a failure initiation point in certain elevated stress situations. This could be caused by stress causing deformation of the filler metal while the base metal is not deformed. The crack tip could then become a stress concentration point once again.

It should be noted however that in other situations this property may actually improve joint performance. In situations such as boiler valves, the repair objective is to prevent further crack growth. Because the cracks grow due to a stress corrosion mechanism, isolating the crack root from the corrosive environment should be sufficient to prevent further crack growth. In this situation, having a ductile repair with sufficient

room to deform has the possibility to extend the life of the repair by deforming during

stressful events such as thermal cycles instead of failing.

3.8 Proposed Composite Brazing

One technique that has potential to alleviate some of the limitations of the current

repair technique is composite brazing. The basic principle of composite brazing is to use

a reinforcement within a brazed joint in order to improve joint properties. The

reinforcement is made of a material with a higher melting point than the filler metal and

is not melted during the brazing process. As a result of this characteristic, it is common

to use a reinforcement of a similar composition to the base metal being brazed. The

reinforcement is placed within the joint before brazing begins and then the filler metal

flows into and around the reinforcement.

Multiple types of reinforcement are currently being investigated such as powders

and porous metals. Powders are advantageous because they can easily fill complex joint

geometries and are simple to use. However, powders are difficult to use in out-of-

position joints without further processing considerations. Porous metals require more

preparation for use but may be able to improve positioning requirements for ultra-wide

gap crack brazing. [16]

For use in a crack brazing situation porous metal would first be formed into a

negative of the crack being filled as illustrated in Figure 3.29. The porous metal must be

made so that significant open porosity exists. The creation of a Mikrosil^{TM} cast of the

crack could be very useful in the creation of this negative. When the crack geometry is exceptionally simple, the porous metal could then be inserted into the crack and retained using a clamping system. Finally, the crack would be brazed using the existing crack repair procedure.
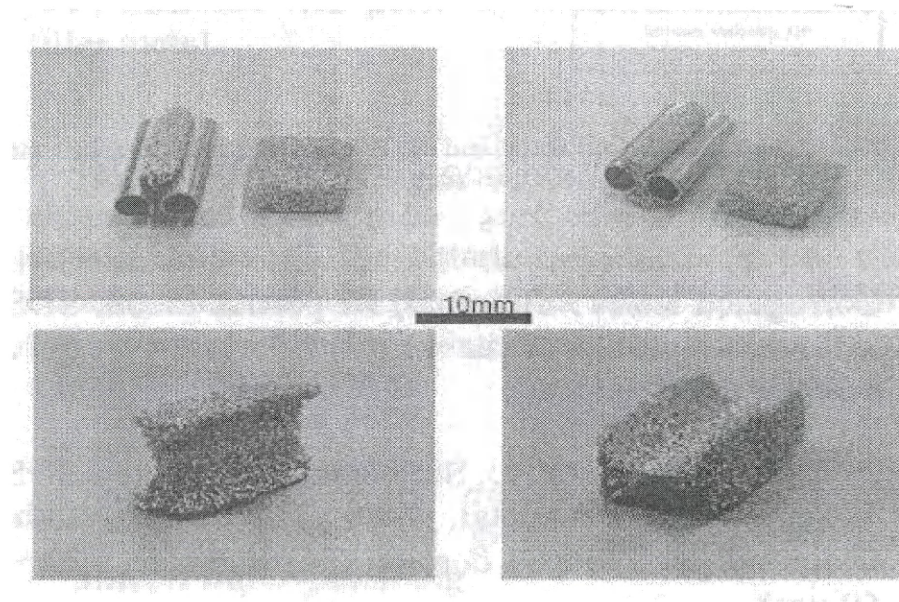
Figure 3.29 Porous metal perform constructed to bridge between
two pipes for brazing [16]

Alternately, a modified powder technique could be used to form the reinforcement in situ as illustrated in Figure 3.30. The proposed technique is to fill the crack with a mixture of carbon and tungsten powders. It is possible that these powders could be applied in a paste form, allowing for easy application to out-of-position cracks. The powders would then be reacted using a combustion synthesis technique to form a porous tungsten carbide structure within the crack. The crack could then be brazed with the existing crack repair procedure. It should be noted that the silver based filler metal currently being investigated for crack repair is commonly used to braze tungsten carbide

to steel in the manufacture of cutting tools due to the fact that the nickel content of the

silver based filler metal improves wetting. [14]

Combustion synthesis is a material production technique which uses the heat

generated from a self-propagating reaction to generate a near net shape part. In this case,

tungsten and carbon powders would be mixed and introduced into the crack. An external

heat source, commonly a tungsten filament, would then initiate the reaction. Because the

formation of tungsten carbide is strongly exothermic, the initial ignition wave then

propagates through the powder mixture. When completed, a porous solidified part is

created in the same shape as the original powder configuration. By adjusting multiple

parameters of the combustion synthesis process, the porosity can be controlled, allowing
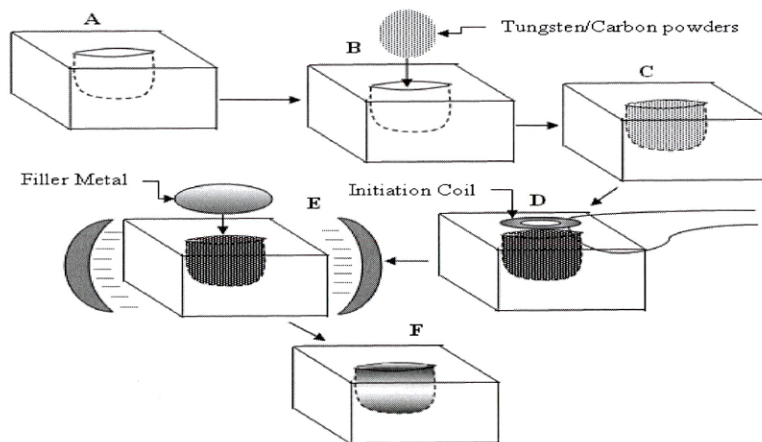
for process optimization.[17]

Figure 3.30 - Illustration of proposed combustion synthesis based composite brazing
crack repair procedure
A- Initial cleaned crack B- Introduction of powder mixture to crack C- Crack filled with
tungsten and carbon powders D- Combustion synthesis reaction creating tungsten
carbide reinforcement E- Brazing F- Completed repair

Predicted advantages of composite brazing are two-fold. First, the porous metal would substantially narrow the effective gap width for brazing. The filler metal would then be able to flow completely through the reinforcement using capillary forces, reaching inaccessible areas and flowing properly in out-of-position brazing. [16]

Secondly, the reinforcement would provide additional strength to the brazed joint in the same way that the reinforcing fibers provide additional strength to more traditional composite materials. Using a reinforcement of similar strength to the base metal would bring the joint properties closer to the properties of the base metal. It is also possible that the composite reinforcement could help restore some of the complex stress states normally associated with brazed joints, however more research is required in this area.

Finally, if the brazing filler metal and the base metal have extensive shared solubility, substantial long term cross-diffusion may be possible, increasing the joint strength substantially. In long-term exposures at elevated temperatures the brazed joint may begin to transform into a partially diffusion bonded joint. This behavior would require at least one of the joint components to have a diffusivity large enough that it could move distances comparable to the diameter of the pores within the composite material. If this diffusion occurs, the strength of the joint can be increased above that of a normal ultra-wide gap brazed joint over the long term.

Overall, the use of composite brazing techniques has the possibility of improving both the capabilities of ultra-wide gap brazing as well as improving the mechanical

properties of ultra-wide gap brazed joints. However, additional research needs to be done

to determine specific processing parameters as well as materials systems best suited for

composite brazing components used for elevated temperature service.

CHAPTER 4

CONCLUSIONS

By examining the entire body of work, several conclusions can be obtained. First, brazing appears to be a viable option for repairing cracks in high temperature boiler valves. However, the cracks in question become ultra-wide gap joints which present specific requirements regarding brazing, both in the joint preparation and crack repair process aspects.

Ultra-wide gap joints have multiple filler metal flow patterns. Surface tension-controlled flow operates when flow velocities are below a threshold determined by the gap width and materials system. When the interface velocity exceeds this threshold, pressure-controlled flow exists. When possible, pressure-driven flow should be avoided in order to avoid the formation of porosity within the joint. In addition, joint geometry can also cause defect formation at the terminal end of certain cracks. Defects can be avoided in smooth joint ultra-wide gap brazing using specific joint design requirements, however it may appear in ultra-wide gap cracks due to the inconsistent crack morphologies which appear.

In boiler valve cracks multiple crack morphologies can occur. From the samples which were examined, it appears that the widest and deepest cracks occur as long cracks which have a very large length-to-depth ratio. In addition, most cracks appear as crack systems, with cracks having multiple branches and intersections with adjacent cracks.

Mikrosil™ casting is effective when characterizing these crack systems and their unique morphologies.

Finally, boiler valve cracks can be effectively cleaned using the higher temperature cleaning procedure detailed in the body of the thesis. While not all oxides may be removed from deep cracks, those cracks can still be cleaned sufficiently so that they can be sealed from the boiler environment. Through brazing, the internal surface of the boiler valve can be isolated from the aggressive environment which will stop the stress corrosion behavior and prevent further damage to the boiler valve.

The crack repair procedure suggested here may be further improved using a composite brazing process using either porous metal or in-situ combustion synthesis composite pre-forms. However as it exists at this moment, the repair procedure is predicted to be effective at repairing ultra-wide gap cracks in high temperature cast steel boiler valves.

REFERENCES CITED

[1] Landrum J., Dennis M. "Ultrasonic Evaluation of Astoria Boiler Circulation Pump Isolation Valve Cracking Letter Report" EPRI NDE Center

[2] Cleaning of Cracked Drum Surfaces for Brazing Repairs, K. Coleman. EPRI, Palo Alto California.

[3] "Brazing Handbook" 4th ed. American Welding Society, 1991.

[4] Milner D. R. "A Survey of the Scientific Principles Related to Wetting and Spreading" *British Welding Journal*, March, 1958

[5] J.O. Hirshfelder, C.F. Curtis and R.B. Bird (1964). *Molecular theory of gases and liquids* (First ed.). Wiley

[6] Lugscheider E. and Iversen K. "Investigations on the Capillary Flow of Brazing Filler Metal BNi5" *Welding Journal,* Oct. 1977

[7] Madeni J. C., Rodas B. and Liu S. 'Effect of filler metal alloying additions in filler metal flow, evaluation of pure copper and BNi-2 filler metals applied to 304 stainless steel base metal's'. Accepted in the IBSC Conference, Orlando, FL., April 26-29, 2009.

[8] Churchill S. W. "Viscous Flows – The Practical Use of Theory" Butterworths, 1988.

[9] Lin W. et al. "Silver braze alloy" United States Patent 6936218. 2005

[10] Yaws C. L. "Chemical Properties Handbook", McGraw Hill, 1999.

[11] Landau L. D. and Lifshitz E. M. "Fluid Mechanics" Pergamon, 1959.

[12] Wilkes J. O. "Fluid Mechanics for Chemical Engineers", Prentice Hall International Series, 1999.

[13] Madeni, J. C. "Investigation of Liquid Filler Metal Flow Process Through a Braze Gap" 2006, p. 165.

[14] Weirauch, D. A. et al. "The spreading kinetics of Ag–28Cu(L) on nickel(S): Part II. Area of spread on surfaces plated with electrolytic Ni" *Journal of Materials Research.* Vol. 12 No. 4 Apr.1997. p. 953.

[15] DeGennes P. G. et al. "Capillarity and Wetting Phenomena" Springer, 2004.

[16] Ariga T et al. "The Effect of the Porous Metal in Ceramics to Metal Brazed Joint". Proceedings of the 4th International Brazing and Soldering Conference, April 26-29, 2009, Hilton in the Walt Disney World Resort, Orlando, Florida, USA. 96-100.

[17] Varma, A Lebrat, J P. "Combustion Synthesis of Advanced Materials". Chemical Engineering Science Volume 47, Issues 9-11, 8 June 1992, Pages 2179-2194

SELECTED BIBILIOGRAPHY

Adams R.D.,The Nondestructive Evaluation of Bonded Structures. Construction & Building Materials Vol. 4 No. 1 March 1990

Ambrose J.C., Nicholas M.G., Stoneham A.M., Dynamics of braze spreading, Acta metall. mater. Vol. 40 No. 10 pp. 2483-2488. 1992.

Chan H.Y., Liaw D.W., Shiue R.K., Microstructural evolution of brazing Ti–6Al–4V and TZM using silver-based braze alloy. Materials Letters 58 (2004) 1141– 1146

Du Y.C., Shiue R.K., Infrared brazing of Ti–6Al–4V using two silver-based braze alloys, Journal of Materials Processing Technology 209 (2009) 5161–5166.

Egbewande A.T., Chukwukaeme C., Ojo O.A., Joining of superalloy Inconel 600 by diffusion induced isothermal solidification of a liquated insert metal. Materials Characterization 59 (2008) 1051–1058

Gottschall R. J., Fundamental scientific research on interfaces in the US Department of Energy's Materials Sciences and Engineering program. Journal of the European Ceramic Society 23 (2003) 2741–2745.

Heiple C., Bennett W., Rising T., Embrittlement of Several Stainless Steels by Liquid Copper and Liquid Braze Alloys. Materials Science and Engineering, 52 (1982) 277-289.

Lee J.G., Kim G.H., Lee M.K., Rhee C.K., Intermetallic formation in a Ti–Cu dissimilar joint brazed using a Zr-based amorphous alloy filler. Intermetallics 18 (2010) 529–535

Molleda F., Mora J., Molleda J.R., Carrillo E., Mora E., Mellor B.G., Copper coating of carbon steel by a furnace brazing process using brass as the braze. Materials Characterization 59 (2008) 613–617

Palanisamy B., Upadhyaya A., Anand K., Evaluation of braze bonded hard complex boride based coatings for sliding, erosion and abrasion wear. Wear 266 (2009) 1058–1065.

Saiz E., Tomsia A.P., Kinetics of high-temperature spreading. Current Opinion in Solid State and Materials Science 9 (2005) 167–173.

Shiue R.K., Wu S.K., Chan C.H., The interfacial reactions of infrared brazing Cu and Ti with two silver-based braze alloys. Journal of Alloys and Compounds 372 (2004) 148–157

Shiue R.K., Wu S.K., Chen S.Y., Infrared brazing of TiAl intermetallic using BAg-8 braze alloy. Acta Materialia 51 (2003) 1991–2004.

Tian J., Kim T., Lu T.J., Hodson H.P., Queheillalt D.T., Sypeck D.J., Wadley H.N.G., The effects of topology upon fluid-flow and heat-transfer within cellular copper structures. International Journal of Heat and Mass Transfer 47 (2004) 3171–3186.

Webb E.B. III, Hoyt J.J., Grest G.S., High temperature wetting: Insights from atomistic simulations. Current Opinion in Solid State and Materials Science 9 (2005) 174–180.

Webb III E.B., Hoyt J.J., Molecular dynamics study of liquid metal infiltration during brazing. Acta Materialia 56 (2008) 1802–1812.

Wu X.W., Chandel R. S., Seow H.P., Li H., Wide gap brazing of stainless steel to nickel base superalloy. Journal of Materials Processing Technology 113 (2001) 215-221

Yang P., Turman B.N., Glass S.J., Halbleib J.A., Voth T.E., Gerstle F.P., Mckenzie B., Clifford J.R., Braze microstructure evolution and mechanical properties of electron beam joined ceramics, Materials Chemistry and Physics 64 (2000) 137–146.

You J.H., Breitbach G., Deformation of ductile braze layer in a joint element under cyclic thermal loads. Fusion Engineering and Design 38 (1998) 307–317.

APPENDIX
SUMMARY OF REPAIR PROCEDURES

1. Determine areas to be repaired using ultrasonic examination
2. Isolate area for cleaning
3. Clean cracked area
    a. Remove all surface oxides using wire brush and compressed air
    b. Immerse cracked surface in 3% hydrogen peroxide for 5 minutes or less
    c. Rinse hydrogen peroxide from surface
    d. Prepare cleaning solution containing 3%hydrogen peroxide and DTPA
        i. Adjust pH to between 8 and 9 using ammonium hydroxide and maintain pH for remainder of cleaning step
    e. Immerse cracked surface in DTPA solution and heat to 80°C
        i. Change DTPA solution when it becomes visually opaque
        ii. Carry out cleaning for 30 hours minimum, however clean longer if cleaning solution changes color in final 30 minutes of cleaning
    f. Rinse cracked surface in room temperature citric acid
    g. Rinse cracked surface in pure water
    h. Dry surface with compressed air
4. Prepare cast of cracked surface
    a. Mix Mikrosil™ casting material according to package instructions
    b. Using wooden spatula work casting material into surface
    c. Wait until cast is solidified
    d. Remove cast from cracked surface using dental pick
    e. Evaluate cast to determine required volume of filler metal
5. Braze cracks
    a. Place potassium fluoride based brazing flux on surface
    b. Work flux into cracks
    c. Heat surface using oxy-fuel torch
        i. Depending on valve wall thickness multiple torches may be required to reach brazing temperature
    d. When brazing temperature is reached introduce BAg-22 filler metal rod to center of heated area
    e. When cracks are filled remove heat and allow valve to cool
6. Evaluate repair quality using phased array ultrasonic examination